Preservation of Garnet Growth Zoning and the Duration of Prograde Metamorphism

Caddick, Mark J ; Konopásek, Jiří ; Thompson, Alan B

Abstract: Chemically zoned garnet growth and coeval modification of this zoning through diffusion are calculated during prograde metamorphic heating to temperatures of up to 850°C. This permits quantification of how the preservation or elimination of zoning profiles in garnet crystals of a given size is sensitive to the specific burial and heating (P-T) path followed, and the integrated duration spent at high temperature (dT/dt). Slow major element diffusion in garnet at T < 600°C means that centimetre-scale zoning profiles may remain for >30 Myr at amphibolite-grade conditions, but small-scale (tens of micrometres) zoning features will be lost early in the prograde stage unless this is 'rapid' (5 Myr for rocks reaching c. 600°C). Calculations indicate that preservation of unmodified growth compositions in even relatively large (up to 3 mm diameter) pelitic garnet crystals requires prograde and exhumational events to be <10 Myr for rocks reaching c. 600°C. This timescale can be 5 Myr for garnet in rocks reaching 650°C or hotter. It is likely, therefore, that most natural prograde-zoned crystals record compositions already partially re-equilibrated between the time of crystal growth and of reaching maximum temperature. However, a large T-t window exists within which crystals begin to lose their growth compositions but retain evidence of crystal-scale zoning trends that may still be useful for thermobarometry purposes. The upper limit of this window for 500 m diameter crystals can be as much as several tens of millions of years of heating to c. 700°C. Absolute re-equilibration timescales can be significantly different for garnet growing in different rock compositions, with examples of a granodiorite and a pelite given

DOI: https://doi.org/10.1093/petrology/egq059

JOURNAL OF PETROLOGY | VOLUME 51 | NUMBER 11 | PAGES 2327–2347 | 2010 | doi:10.1093/petrology/egq059

Preservation of Garnet Growth Zoning and the Duration of Prograde Metamorphism

MARK J. CADDICK[1]*, JIŘÍ KONOPÁSEK[2] AND ALAN B. THOMPSON[1,3]

[1]INSTITUTE FOR MINERALOGY AND PETROLOGY, ETH ZÜRICH, CLAUSIUSSTRASSE 25, NW, 8092 ZÜRICH, SWITZERLAND

[2]CZECH GEOLOGICAL SURVEY, KLÁROV 3, 118 21 PRAHA 1, CZECH REPUBLIC

[3]FACULTY OF SCIENCE, UNIVERSITY OF ZÜRICH, ZÜRICH, 8057 SWITZERLAND

RECEIVED NOVEMBER 24, 2009; ACCEPTED SEPTEMBER 7, 2010

*Chemically zoned garnet growth and coeval modification of this zoning through diffusion are calculated during prograde metamorphic heating to temperatures of up to 850°C. This permits quantification of how the preservation or elimination of zoning profiles in garnet crystals of a given size is sensitive to the specific burial and heating (*P–T*) path followed, and the integrated duration spent at high temperature (dT/dt). Slow major element diffusion in garnet at* $T < 600°C$ *means that centimetre-scale zoning profiles may remain for >30 Myr at amphibolite-grade conditions, but small-scale (tens of micrometres) zoning features will be lost early in the prograde stage unless this is 'rapid' (≪5 Myr for rocks reaching* c. *600°C). Calculations indicate that preservation of unmodified growth compositions in even relatively large (up to 3 mm diameter) pelitic garnet crystals requires prograde and exhumational events to be <10 Myr for rocks reaching* c. *600°C. This timescale can be ≪5 Myr for garnet in rocks reaching 650°C or hotter. It is likely, therefore, that most natural prograde-zoned crystals record compositions already partially re-equilibrated between the time of crystal growth and of reaching maximum temperature. However, a large* T–t *window exists within which crystals begin to lose their growth compositions but retain evidence of crystal-scale zoning trends that may still be useful for thermobarometry purposes. The upper limit of this window for 500 μm diameter crystals can be as much as several tens of millions of years of heating to* c. *700°C. Absolute re-equilibration timescales can be significantly different for garnet growing in different rock compositions, with examples of a granodiorite and a pelite given.*

KEY WORDS: *garnet; diffusion; geochronology; metamorphism; thermobarometry*

INTRODUCTION

Isotopic, structural and petrological studies have shown the duration of some orogenic events to be at least an order of magnitude shorter than previously thought (<2 Myr rather than >20 Myr; e.g. O'Brien & Vrana, 1995; Dewey, 1997; Perchuk & Philippot, 1997; Dewey & Mange, 1999; Oliver *et al.*, 2000; Rubatto & Hermann, 2001; Zulauf *et al.*, 2002; Camacho *et al.*, 2005; Ague & Baxter, 2007). The previously 'slow' rates arose from the assumption that both burial and exhumation processes proceeded uniformly at the rates inferred for erosion (e.g. 0·1–0·5 mm a^{-1}, 'slow Barrovian' in Fig. 1). Faster rates suggest that additional processes or special tectonic geometries must be considered, especially those facilitating rapid exhumation of deeply buried rocks (e.g. extrusion tectonics at plate-tectonic speeds). An improved knowledge of the duration of heating and cooling intervals in various metamorphic settings can help to reveal these processes of orogenic development, but rates of metamorphism are usually difficult to discern accurately. Specifically, despite advances in mineral cooling thermochronology for calibrating exhumation histories [see review by Reiners *et al.* (2005) and companion papers in that volume], estimation

*Corresponding author: Telephone: +41 44 632 7991. Fax: +41 44 632 1636. E-mail: mark.caddick@erdw.ethz.ch

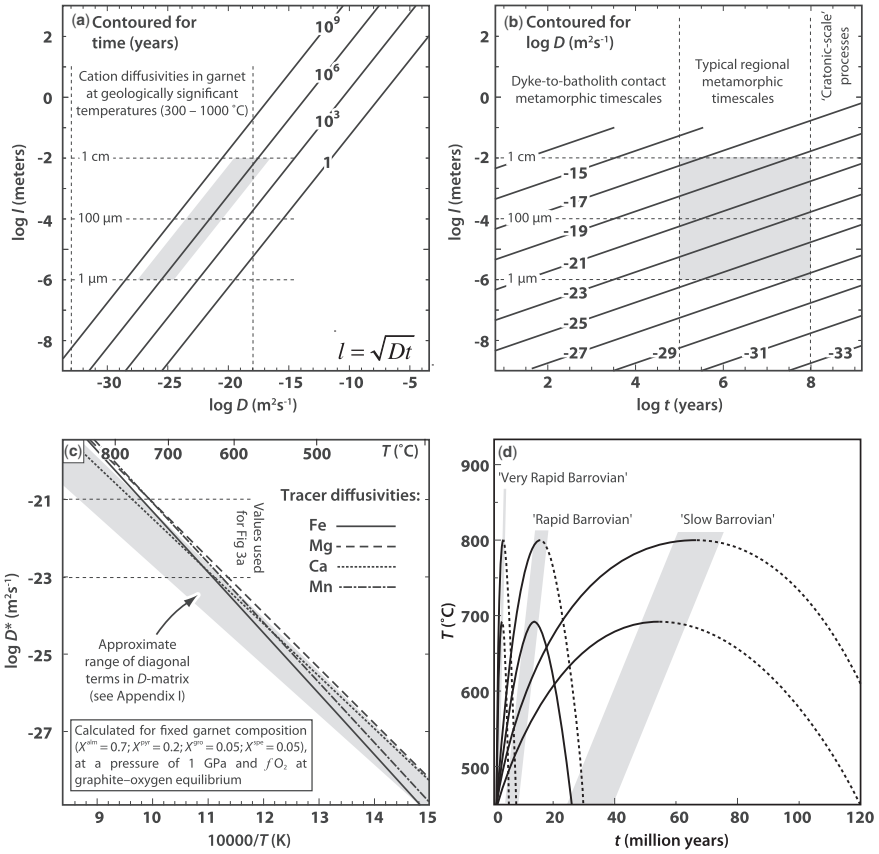

Fig. 1. Characteristic length-scale and time-scaling relationships ($l^2 = nDt$) appropriate for cation diffusion in garnet at metamorphic temperatures (300–1000°C). (a) Effective diffusion length ($\log_{10}l_{eff}$) as a function of diffusivity ($\log_{10}D$), contoured for time (1 year to 1 Ga). Range of typical metamorphic grain sizes (*c.* 1 µm to 1 cm) and garnet diffusivities ($\leq 10^{-18}$ m^2 s^{-1}) indicated by dashed lines. (b) Diffusion length ($\log_{10}l_{eff}$) as a function of time [$\log_{10}t$ (years)], contoured for diffusivity ($\log_{10}D$). Range of typical metamorphic grain sizes and timescales indicated by dashed lines. Grey fields in (a) and (b) indicate l_{eff}–t–D range most appropriate for crystals experiencing Barrovian-type metamorphism ($T_{Max} \approx 700$°C, duration up to several tens of millions of years, crystal sizes between 1 µm and 1 cm). (c) Fe, Mg, Ca and Mn tracer diffusivities in garnet as a function of temperature, calculated with data from Carlson (2006) for a pelitic garnet at fixed P and oxygen fugacity (Appendix I). Grey band indicates approximate range of diagonal terms in the coupled multi-component diffusion matrix (calculated after Lasaga, 1979; see Appendix I). (d) Continuous-line curves show examples of three possible but distinct timescales of heating associated with Barrovian-style metamorphism (i.e. chiefly associated with crustal thickening not contact metamorphism). Based upon crustal heat modelling and petrologically constrained results which suggest 'very rapid' (Ague & Baxter, 2007), 'rapid' (Harrison *et al.*, 1998) or 'slow' (Thompson & England, 1984) metamorphism. Dotted lines indicate simple continuation as exhumation paths after T_{Max}, at similar rates.

of prograde metamorphic rates remains challenging (Vance & O'Nions, 1990; Christensen *et al.*, 1994; Foster *et al.*, 2004).

Zoned minerals, with different patterns of chemical profiles for different elements, have been reported from a wide variety of metamorphic and magmatic rocks. They have frequently been used to infer orogenic pressure–temperature (P–T) and fluid histories (e.g. Tracy *et al.*, 1976; Spear & Selverstone, 1983; St-Onge, 1987; Kohn *et al.*, 1997; Inui & Torium, 2002; Harris *et al.*, 2007). Chemical zoning generated during mineral growth is often subsequently modified by diffusional relaxation at temperatures above a nominal diffusional 'closure' temperature range, which for any element is chiefly dependent on cooling rate and grain size (Dodson, 1973). Because of the strong dependence of cation diffusivity upon temperature, there have been numerous attempts aimed at deducing rates and duration of geological (thermal) processes based upon measured zoning profiles in garnet for major and minor elements or isotopes, using so-called geospeedometry (e.g. Lasaga, 1983; Ganguly *et al.*, 1996, 2000; Dachs & Proyer, 2002; Faryad & Chakraborty, 2005; Chakraborty, 2006; Ague & Baxter, 2007). In each case, an initial (pre-diffusion) zoning configuration and approximate T history must be deduced, from which time-dependent diffusive relaxation of gradients can be forward-modelled (e.g. Florence & Spear, 1991, 1993; Gaidies *et al.*, 2008).

The fact that chemical zonation is preserved in some minerals suggests that distinct geological processes typically fall within a specific set of time (t) ranges for a given

temperature range, and that this can be interpreted from the size and nature of preserved intra-crystalline chemical zones. In particular, earlier observations allowed the empirical conclusion that zoning in metamorphic garnet crystals is subject to diffusive relaxation over the timescales of amphibolite-grade metamorphic events (e.g. Anderson & Olimpio, 1977; Woodsworth, 1977; Dempster, 1985). This even led to a proposed 'change-in-garnet zoning-pattern isograd' (Yardley, 1977). The absolute amount of diffusive resetting experienced by crystals of several sizes was calculated by Florence & Spear (1991). They suggested that crystals with radii in the range 0·5–2·5 mm could be particularly susceptible to resetting during cooling from maximum temperatures in the approximate range 500–700°C, depending on cooling rate [summarized in fig. 12 of Florence & Spear (1991)]. Here we describe approaches based upon calculations of prograde chemical zoning to refine these T–t limits. From this the duration of successively recorded metamorphic events may be inferred. Both analytical and numerical methods are presented here, with the former providing valuable scaling analysis of diffusion problems applied to metamorphic garnet and the latter coupling thermodynamically constrained growth zoning profiles to a finite-difference model for diffusional relaxation of intra-crystalline chemical gradients. We focus particularly on prograde metamorphism of different durations, with results revealing information on the relationship between multi-component patterns of diffusion-modified garnet zoning and the duration of metamorphic heating episodes. We have calculated the likely range of dT/dt required to preserve prograde growth compositions up to metamorphic peak conditions (T_{Max}) in natural environments experiencing different rates of metamorphism. This indicates the circumstances in which apparent prograde garnet zoning may be safely used for thermobarometry to constrain parts of the burial and heating P–T history and reveals the far larger range of conditions under which original growth compositions are significantly modified during prograde metamorphism. This distinction is important because we show that in many cases it is possible to preserve crystal-scale growth zoning trends over protracted P–T–t histories, but with loss of any record of the actual growth compositions long before peak temperature is reached.

DIFFUSION LENGTH AND TIMESCALES REQUIRED TO GROW AND PRESERVE ZONED MINERALS

The generation and preservation of chemically zoned crystals requires that the length-scale over which diffusion operates in the time available is smaller than that over which the driving chemical (or chemical potential) gradients occur. With the assumption of static crystal boundaries and a simple isothermal history, the timescales required for relaxation of such chemical gradients over crystal length-scales at metamorphic temperatures can be evaluated for numerous elements and their isotopes with either analytical or numerical approaches (e.g. Chakraborty & Ganguly, 1991; Florence & Spear, 1991; Cherniak *et al.*, 2004; Watson & Baxter, 2007). Well-known analytical solutions allow simple estimation of the diffusivity–time–length (D–t–l) relationships appropriate for the preservation or loss of chemical gradients by analogy with heat flow (e.g. Crank, 1956; Carslaw & Jaeger, 1959). These yield several types of diagrams that are useful for illustrating the D–t–l relationships most suitable for retrieving timescale information from metamorphic rocks, and are briefly reviewed next.

Parameter ranges required to preserve zoned minerals

The effective diffusion length is a well-known tool for assessing the approximate length-scale over which chemical gradients will be relaxed for any particular duration (e.g. Spear & Florence, 1992). This can be defined as $l_{eff} = n\sqrt{(Dt)}$ (e.g. Darken & Gurry, 1953, p. 447), where D, t and n are respectively diffusivity, time, and a constant depending upon geometry (for illustration we use $n = 1$ here). l_{eff} is analogous to the thermal conduction length-scale as a function of time and thermal diffusivity (e.g. Spear, 1993), stating the distance to the point where a certain amount of the initial compositional difference across a compositional step has been lost by diffusion. At a constant diffusivity of $1 \times 10^{-18}\,m^2\,s^{-1}$ an effective diffusion length of 1 cm is reached in *c.* 1 Myr whereas a 10 μm length is achieved in only about 1 year (Fig. 1a). Low diffusivities increase the time to length-squared ratio accordingly, such that at $1 \times 10^{-30}\,m^2\,s^{-1}$ an effective diffusion length-scale as short as 1 μm requires of the order of 1 billion years. Thus small-scale (1–10 μm) zoning can essentially remain unmodified over billion year timescales at diffusivities below $10^{-27}\,m^2\,s^{-1}$ but would be modified in hundreds to thousands of years at diffusivities above $10^{-21}\,m^2\,s^{-1}$ (Fig. 1b). Conversely, centimetre-scale zoning can withstand billion year timescales at diffusivities less than *c.* $10^{-22}\,m^2\,s^{-1}$, with large-scale chemical communication effectively impossible for lower diffusivities or shorter timescales. This extreme range of l_{eff} as a function of varying D suggests that analysis of diffusion profiles for multiple elements with significantly different D values (e.g. divalent and trivalent cations within the same crystal) can reveal evidence of short duration thermal events superimposed upon longer term or poly-metamorphic histories. More generally, as calibration of diffusion coefficients for a wider range of elements and crystal systems becomes available, it will increasingly be possible to use the specific diffusion data for (major or trace) elements that most

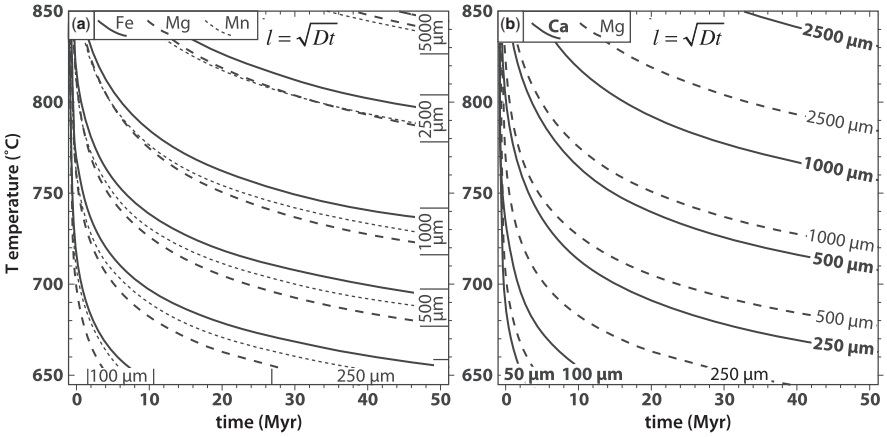

Fig. 2. Analytical solution of the effective diffusion length, $l = \sqrt{Dt}$, contoured to represent the length-scale at which (and below which) cation diffusion in garnet is significant for any T–t condition. (a) Contours for Fe, Mg and Mn tracer diffusivities at seven lengths (100 μm to 5 mm). (b) Contours calculated using Ca tracer diffusivities (Mg curves shown for comparison). All contours calculated for a fixed garnet composition ($Alm_{0·7}Pyr_{0·2}Gro_{0·05}Spe_{0·05}$, as Fig. 1c) using the D–T data of Carlson (2006) (see Appendix I).

precisely record interpretable chemical zoning in natural samples.

Diffusion length and timescales appropriate for zoning in garnet

For regional metamorphic timescales (*c.* 10^5–10^8 years, Fig 1d), typical garnet grain sizes (1 μm to 1 cm) are approximately of the order of the effective diffusion length if D is in the range 10^{-17}–10^{-28} m^2 s^{-1} (shaded region in Fig. 1a and b). Diffusivity is strongly temperature dependent, with divalent cation (Fe, Mn, Mg and Ca) diffusivities of 10^{-17}–10^{-28} m^2 s^{-1} in garnet requiring a broad temperature range of *c.* 400–1150°C (Fig. 1c). The maximum cation diffusivity over the more typical metamorphic temperature range of 400–700°C is 10^{-21} m^2 s^{-1}, clearly implying a simple temperature–duration relationship in which smaller crystals lose their zoning by diffusion during regional metamorphism whereas larger ones can retain primary compositions (e.g. Florence & Spear, 1991; Spear *et al.*, 1991; Stüwe & Ehlers, 1996; Gaidies *et al.*, 2008). Figure 2 illustrates this, contouring T–t space for l_{eff} to explicitly demonstrate the Arrhenian dependence of D on T [see also Fig. 1c and Appendix I, equation (6)]. Contours in Fig. 2 suggest, for example, that garnet zoning over 500 μm length-scales (be that whole-crystal core–rim zoning or more complex internal zoning established during growth or surrounding inclusions) would undergo substantial re-equilibration if held at 750°C for 10 Myr. Compositional heterogeneities over order of magnitude longer length-scales remain effectively unmodified under the same conditions. As described elsewhere (e.g. Jiang & Lasaga, 1990; Ague & Baxter, 2007) small zoning features such as <100 μm diameter crystals or single compositional steps within larger zoning profiles would be subject to very rapid relaxation, and their preservation is thus indicative of very short duration (<10^5 years) metamorphic events. At intermediate T–t–l_{eff} ranges (e.g. a chemical gradient over 250 μm held at 700°C for 10 Myr), different tracer diffusivity values result in partial re-equilibration of only the fastest-diffusing elements (here assuming that diffusions of Mg and Ca are independent; Fig. 2b).

Diffusional progress as a function of length and time

The effective diffusion length is useful for estimating the distance over which diffusion operates in a given time. However, for many petrologically relevant problems it is more valuable to know the amount of compositional change that will occur after a given time at any distance from an initial compositional heterogeneity. Specifically, it is useful to know whether a zoned crystal is likely to preserve its original or a substantially diffusion-modified zoning profile, and whether an unzoned crystal is likely to represent a lack of zoning established during growth or almost-complete diffusive re-equilibration. We discuss below the implications of these end-member cases for quantitative determination of pressure, temperature and time history.

For a spherical and initially homogeneous crystal surrounded by a compositionally different matrix (or a matrix whose K_D of the component of interest is out of equilibrium with the crystal), the concentration of any component can be expressed as a function of position within the crystal and time by assuming that the matrix composition is fixed. One assumes further that no kinetic or exchange barrier retards communication between matrix and crystal, that the diffusion coefficient is constant

through time (i.e. independent of composition at a fixed temperature), and that diffusion of multiple elements is not coupled (as in tracer diffusion).

$$C_{t,r} = C_0 + (C_m - C_0) \times \left[1 + \frac{2a}{\pi r} \sum_{n=1}^{\infty} \frac{-1^n}{n} \cdot \sin \frac{n\pi r}{a} \cdot \exp\left(-Dn^2\pi^2 \, t/a^2\right) \right] \quad (1)$$

where $C_{t,r}$ is the resultant component concentration at radial position r within the spherical crystal of radius a, C_0 is the initial uniform concentration within the crystal, and C_m is the constant matrix composition (Crank, 1956). The concentration at the crystal core is given by

$$C_t = C_0 + (C_m - C_0)\left[1 + 2 \sum_{n=1}^{\infty} -1^n \cdot \exp\left(-Dn^2\pi^2 \, t/a^2\right) \right]. \quad (2)$$

Compositional change proceeds inwards from the crystal rim at a rate dependent on the initial compositional difference ($C_0 - C_m$), crystal size (a) and diffusivity (D). 'Diffusion completeness' can thus be expressed as the proportion of the change from C_0 to C_m that has occurred at any position in the crystal after any time (the crystal will tend to a uniform composition of C_m at infinite time). This parameter, $(C_{t,r} - C_0)/(C_m - C_0)$, is particularly useful because a calculated 'diffusion completeness' value is valid for any given absolute initial difference between crystal and matrix composition (for the conditions listed above). This provides a generalized scheme for predicting the extent of compositional change as a result of diffusion. Here we consider diffusion coefficients to be insensitive to crystal composition, using the composition-dependent data and formulation of Carlson (2006) but at a fixed almandine-rich composition. Composition-dependent diffusivities, simultaneous crystal growth and diffusion, and temperature-dependent equilibrium crystal rim compositions are addressed explicitly in numerical simulations, below.

Contours of diffusion completeness as a function of time and position within a spherical crystal, calculated with equation (1) for grain sizes of typical metamorphic garnet, are shown in Fig. 3. This suggests (Fig. 3a) that after 10^5 years an initially unzoned 1 mm diameter crystal undergoing absorption at its rim of a component with a diffusivity of $10^{-21}\,m^2\,s^{-1}$ (see lower set of x-axis scales, Fig. 3a) will be highly zoned. This garnet has effectively experienced no change of its core composition, but an *c.* 25% shift from C_0 to C_m 0·4 mm from the crystal core, and a *c.* 90% shift towards the matrix composition 0·49 mm from the core (10 μm from the rim). A crystal under the same conditions for 1 Myr would experience a significant change of its core composition, reaching *c.* 45% towards C_m from C_0. In this case, the 90% 'diffusion completeness' contour penetrates *c.* 70 μm in from the crystal rim and a *c.* 99% shift from C_0 to C_m is experienced at the point 10 μm from the crystal rim. Diffusion completeness profiles as a function of distance from core to rim of this 1 mm diameter crystal after 10^3, 10^4, 10^5, 10^6 and 10^7 years are shown in Fig. 3b, illustrating that near-rim compositions are subject to change over very short timescales (tens of years for the chosen D value of $10^{-21}\,m^2\,s^{-1}$), whereas core compositions are preserved for several orders of magnitude longer. The duration over which the initial crystal core composition would be maintained has been tabulated for a range of typical crystal sizes and temperatures (Table 1), based upon the assumptions of constant T and C_m discussed above. As illustrated below with a numerical simulation, this is a maximum duration, with pre-existing internal zoning profiles dramatically shortening timescales of crystal core partial re-equilibration. Figure 3b can also be reformulated with dimensionless variables for position (r/a) and the contoured variable (Dt/a^2), as illustrated by Carslaw & Jaeger (1959, p. 234) and reproduced by Crank (1975, p. 92).

Diffusion completeness contours calculated for Fe within 1 mm and 1 cm diameter garnet crystals are shown as a function of time and temperature in Fig. 3c and d. In each case, contours representing diffusion completeness in the crystal core and at a point 20 μm from the rim are shown, with increasing temperature decreasing the duration required to reach a particular degree of diffusion completeness at either position. For example, a 1% change from C_0 to C_m in the near-rim of the 1 mm diameter crystal (Fig. 3c) is achieved after 10^4 years at *c.* 680°C, 10^5 years at *c.* 620°C, 10^6 years at 570°C or 10^7 years at 520°C. The position of this very low (1%) diffusion completeness contour is essentially independent of crystal size (compare, for example, un-dashed 1% contours at lower left of Fig. 3c and d), because in each case this effectively records only a diffusion penetration depth of 20 μm from the absolute crystal rim. The time required for the near-rim of a crystal to reach a higher order of diffusion completeness (e.g. >80%) is more clearly crystal-size-dependent, so that the near-rims of larger crystals (e.g. Fig. 3d) spend a longer duration at intermediate levels of diffusion completeness for any given T than smaller crystals (e.g. Fig. 3c). This follows closely from the volume to surface-area ratio for a spherical crystal, with the strong grain-size dependence of the total amount of material absorbed by the crystal described for the set of assumptions listed above by Crank (1975, equation 6.20):

$$\frac{M_t}{M_\infty} = 1 - \frac{6}{\pi^2} \sum_{n=1}^{\infty} \frac{1}{n^2} \cdot \exp\left(-Dn^2\pi^2 \, t/a^2\right) \quad (3)$$

where M_t is the amount of material absorbed until and including time t, normalized to the total amount of material that will have been absorbed as $t \to \infty$. Relationships between M, D, t and a are shown graphically in the

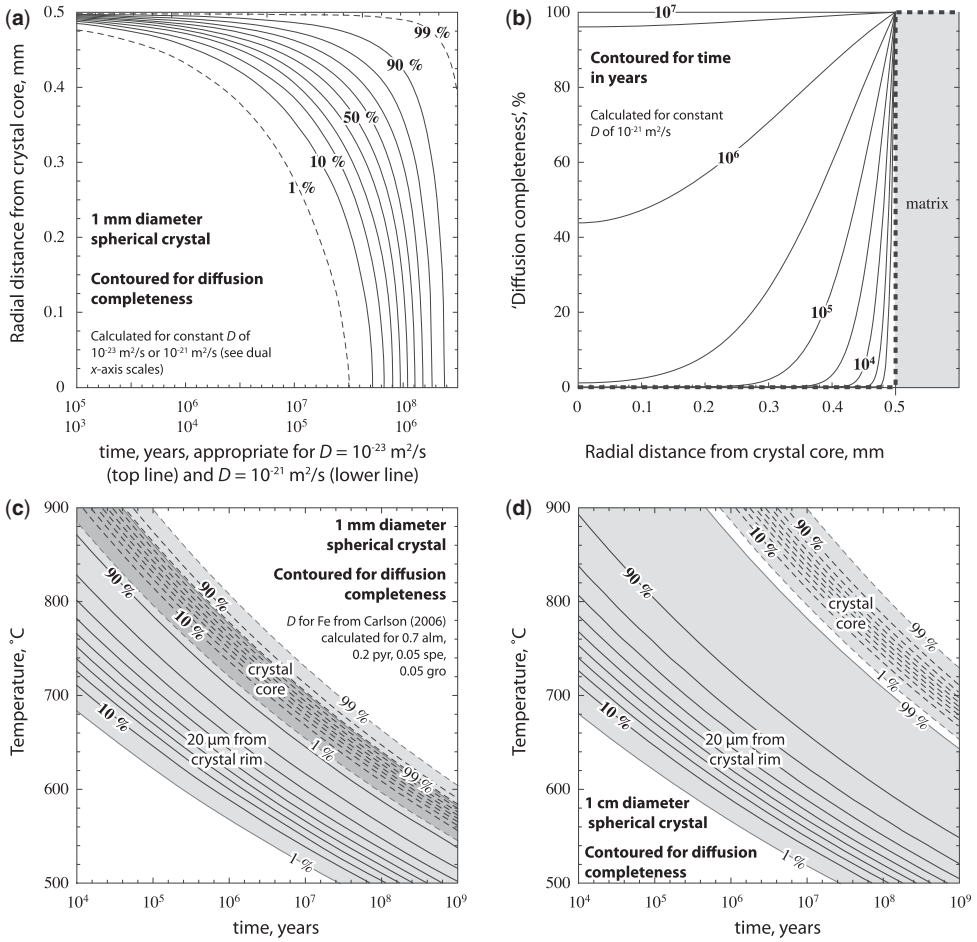

Fig. 3. (a) Calculated diffusion completeness as a function of time and radial distance through an initially homogeneous 1 mm diameter spherical crystal; 1% and 99% completeness shown with dashed curves, 10% interval contours shown with continuous contours. It should be noted that the *x*-axis is labelled with dual scales, with top and bottom appropriate for diffusivities of 10^{-23} and 10^{-21} m s^{-1}, respectively. (b) Diffusion completeness profiles through the same 1 mm diameter crystal as in (a), here contoured for diffusion durations in the range 10^3–10^7 years. It should be noted that here the matrix composition is fixed over time. (c) Diffusion completeness as a function of temperature and time at two positions in a 1 mm diameter crystal. Continuous contours show diffusion completeness 20 μm from the crystal rim; dashed contours show completeness in the crystal core (1% and 99% contours are drawn for each, as are 10% interval contours in the range 10–90%). For both core and near-rim, the region bounded by the 1 and 99% completeness contours is shaded pale grey (dark grey where the two regions overlap; i.e. *T*–*t* regions in which the crystal core reaches >1% completeness whereas the near-rim point has not exceeded 99% completeness). (d) as (c) but for a 1 cm diameter crystal.

Supplementary Data to this paper (available at http://www.petrology.oxfordjournals.org/).

Although the near-rim of a 1 mm diameter crystal rapidly experiences 1% diffusion completeness at high temperature (Fig. 3c), as also implied by Fig. 3a and b it takes more than two orders of magnitude longer for this change to significantly affect the crystal core (*c.* $10^{6\cdot5}$ years at 680°C). This time difference essentially records the duration between opening of first the crystal rim and then its core to significant modification by diffusion. The length of this delay is a scalable function of crystal size, as demonstrated by comparison with an order of magnitude larger (1 cm diameter) crystal in which the rim reaches 99% diffusion completeness before the core reaches 1% completeness (Fig. 3d). However, because initial changes to the near-rim composition of crystals with radii larger than *c.* 100 μm are effectively insensitive to crystal size and occur significantly faster than initial changes to crystal core composition, the duration of this delay can readily be approximated over a range of crystal sizes and metamorphic temperatures by simply calculating the time of initial core-resetting [e.g. with equations (2) and (6); Fig. 4]. For species with diffusion coefficients similar to that of Fe in garnet, this serves as a guide to how long a spherical crystal can reside in chemical disequilibrium with the matrix at high temperature before the initial

Table 1: Time at which crystal core compositions are first modified*

Temperature	*D*	Diameter (mm)					
(°C)	(m^2 s^{-1})†	0·05	0·10	0·50	1·00	5·00	10·00
550	$4{\cdot}028 \times 10^{-25}$	6·039	6·641	8·039	8·641	10·039	10·641
600	$3{\cdot}730 \times 10^{-24}$	5·073	5·675	7·073	7·675	9·073	9·675
650	$2{\cdot}714 \times 10^{-23}$	4·211	4·813	6·211	6·813	8·211	8·813
700	$1{\cdot}610 \times 10^{-22}$	3·438	4·040	5·438	6·040	7·438	8·040
750	$8{\cdot}026 \times 10^{-22}$	2·740	3·342	4·740	5·342	6·740	7·342
800	$3{\cdot}445 \times 10^{-21}$	2·107	2·709	4·107	4·709	6·107	6·709
850	$1{\cdot}299 \times 10^{-20}$	1·531	2·133	3·531	4·133	5·531	6·133

*Log_{10} of time (in years) at which diffusion completeness in crystal core first exceeds 0·01% if held at temperature in left column, calculated with equation (2).
†Diffusion coefficients calculated at *T* with Fe data of Carlson (2006) and crystal composition as in Fig. 3c and d ($Alm_{0·7}Pyr_{0·2}Spe_{0·05}Gro_{0·05}$).

composition of the geometric crystal core is modified by diffusion. Again we emphasize that this records a maximum duration, with pre-existing internal gradients reducing resetting timescales accordingly. Furthermore, it is not straightforward to know whether an analysed crystal core records C_0 or a partially modified composition, although the magnitude and position of chemical gradients within the crystal may help to reveal this. For the example of a previously unzoned crystal not undergoing growth but subject to addition of a component from an infinite reservoir (e.g. Fig. 3b), steep chemical gradients at the rim and shallow gradients in the core reflect low degrees of diffusion completeness ($C_{core} \approx C_0$). The maximum curvature in chemical gradients moves towards the crystal core as diffusion completeness approaches *c.* 20%, and the relative width of this most curved zone continues to increase towards high degrees of diffusion completeness ($C_{core} \rightarrow C_m$).

An implication of the fact that near-rim compositions of all crystals (independent of size) initially respond to an imposed chemical gradient at effectively the same rate is that there is no particular virtue in choosing larger crystals for rim-composition thermobarometry in the hope that they better record peak *P*–*T* conditions. Cessation of garnet growth at or before peak-*T* limits our ability to estimate peak-*T* conditions from natural rocks, as mineral rim compositions (and thus accurate records of K_D of equilibration) begin to reset quickly, regardless of grain size or internal crystal zoning. The apparent temperature recorded is then a sensitive function of initial temperature and cooling rate (Spear, 1991). However, near-rim sections of larger crystals are more resistant to advanced stages of resetting (i.e. diffusion completeness approaching 100%), which may introduce additional error when using near-rim crystal compositions for *P*–*T* estimates of late-stage equilibration with the matrix. Unlike crystal rims, the inner parts of larger crystals would preserve initial compositions for longer than smaller crystals (compare, for example, the dashed 1% contours in Figs. 3c and d, and see Fig. 4), which can clearly be exploited to examine early growth conditions [as described previously by Florence & Spear (1991) and Gaidies *et al.* (2008)].

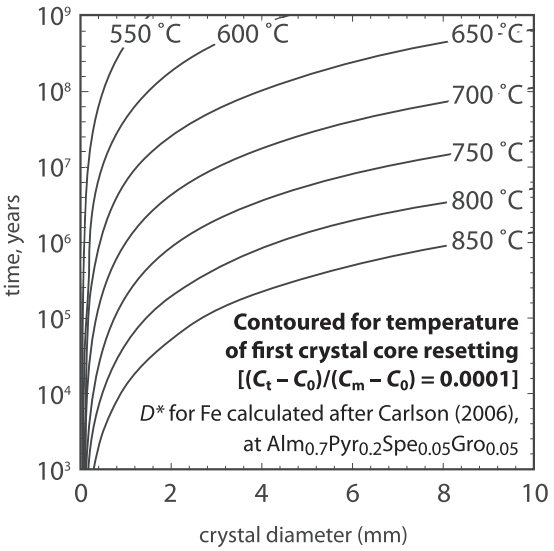

Fig. 4. Calculated temperature–time–crystal-size relationships at which the cores of initially homogeneous spherical garnet crystals first experience compositional change in response to re-equilibration with the rock matrix. Contours represent 0·01% diffusion completeness, calculated with equation (2) using the Fe tracer diffusion data of Carlson (2006).

Figures 3c and d and 4 show log time units rather than the linear scale shown in Fig. 2. Replotting in linear units

reveals two distinct ranges of opening to diffusion. Between 0 and *c.* 10 Myr contours are steep in T–t space for any given grain size, with significant shallowing of the gradient at longer timescales (e.g. Fig. 2). Thus garnet growing during shorter term metamorphic events (<1 to *c.* 5 Myr) will experience partial relaxation of chemical gradients—which is unlikely to completely eradicate zoning, as diffusion completeness is sensitive to small changes in metamorphic duration. Crystals experiencing longer term thermal activity (5–15 Myr) are likely to show extensive relaxation and a significant deviation of all parts of a crystal from their initial compositions, and crystals experiencing >15 Myr metamorphic durations are likely to be substantially modified from their growth compositions, or become completely unzoned. This also implies that the temporal resolution possible with diffusion-modified compositional mapping (geospeedometry) is far lower for long duration metamorphic events than for those of <5 Myr near T_{Max}.

CHEMICAL ZONING IN GARNET FORMED DURING PROGRADE METAMORPHISM

Analytical solutions are well suited for calculation of diffusion in very specific circumstances such as the development of zoning in crystals communicating with an infinite matrix reservoir (e.g. Figs 3 and 4) or relaxation of simple zoning profiles during subsequent metamorphism (e.g. Jiang & Lasaga, 1990). However, development of a diffusion model appropriate for natural metamorphic settings raises several additional challenges not readily described analytically: (1) crystal growth (over a prolonged phase or in multiple distinct events) invalidates any solution requiring fixed boundary positions; (2) changing equilibrium partitioning during a metamorphic cycle (owing to changing intensive variables or metasomatism) challenges the requirement of a constant boundary composition; (3) although the diffusional consequences of a simple polythermal history can be approximated by an isothermal calculation (Chakraborty & Ganguly, 1991; O'Brien, 1997), this still fails to account for grain growth throughout the metamorphic history; (4) diffusion of multiple major elements is not independent, with a flux of one component requiring a counter flux of others; (5) diffusivities can be strongly controlled by crystal composition (Ganguly *et al.*, 1998; Carlson, 2006), which may change dramatically through a metamorphic cycle. These problems can be addressed with a suitable finite-difference diffusion model (e.g. Florence & Spear, 1991; Spear, 1991; Dachs & Proyer, 2002; Storm & Spear, 2005; Gaidies *et al.*, 2008) if the initial compositional gradients ($\Delta X/l$) to be relaxed can also be constrained.

Florence & Spear (1991) and Spear *et al.* (1991) demonstrated that garnet growth zoning can be predicted along a prescribed P–T path with differential thermodynamic constraints. They assumed knowledge of the stable mineral assemblage as a basis for diffusion calculations. Their results (Florence & Spear, 1991) suggested a range of crystal-radius–T_{Max}–heating-rate conditions appropriate for the accurate determination of P–T paths from zoned crystals, based upon isobaric heating ± cooling calculations in the range 485–635°C, and two polybaric P–T calculations reaching a peak temperature of 610°C. Calculations on the effects of cooling equilibrated compositions from metamorphic peak T clearly revealed how apparent temperatures recorded by coexisting mineral compositions in amphibolite-grade (Spear, 1991) and granulite-grade (Spear & Florence, 1992) rocks can be modified by cation-exchange and intra-crystalline diffusion. The amount of modification is a strong function of cooling rate, garnet crystal size and the relative proportions of key phases in the assemblage. In an alternative approach, Gaidies *et al.* (2008) employed Gibbs free energy minimization to establish both the equilibrium mineral assemblage and the composition of garnet along a P–T path. They demonstrated that the sensitivity of growth zoning to diffusional modification varies as a function of the P–T conditions of, and time since, garnet nucleation. In this case, final crystal size was directly correlated with time of crystal nucleation so that differences in any two final crystal zoning profiles produced by a P–T path were a linked function of both the different equilibrium conditions through which they grew (with large crystals experiencing core growth compositions earlier in the history), and the appropriate amount of diffusive relaxation for that crystal size.

Here we also employ a free energy minimization approach to calculate both the stable mineral assemblage and phase compositions for a given bulk-rock composition along a chosen P–T path. We thus calculate the magnitude of chemical gradients formed during garnet growth from the rock matrix and use a finite-difference model of intra-crystalline diffusion to predict their relaxation. We are interested in precisely quantifying relationships between temperature, heating rate, crystal size and the partial or complete loss of whole-crystal zoning during prograde metamorphism, and provide a continuous set of graphical solutions up to granulite conditions for heating paths requiring up to 50 Myr. We examine the chances of preserving crystal-scale growth zoning up to peak metamorphic (T_{Max}) conditions, by mapping out a large range of heating durations, peak temperatures, and crystal sizes (diameters in the range 0·5–10 mm). In particular, we quantify when along a prograde path the compositions of crystal cores are first modified by diffusion, and then when diffusion eventually results in unzoned crystals.

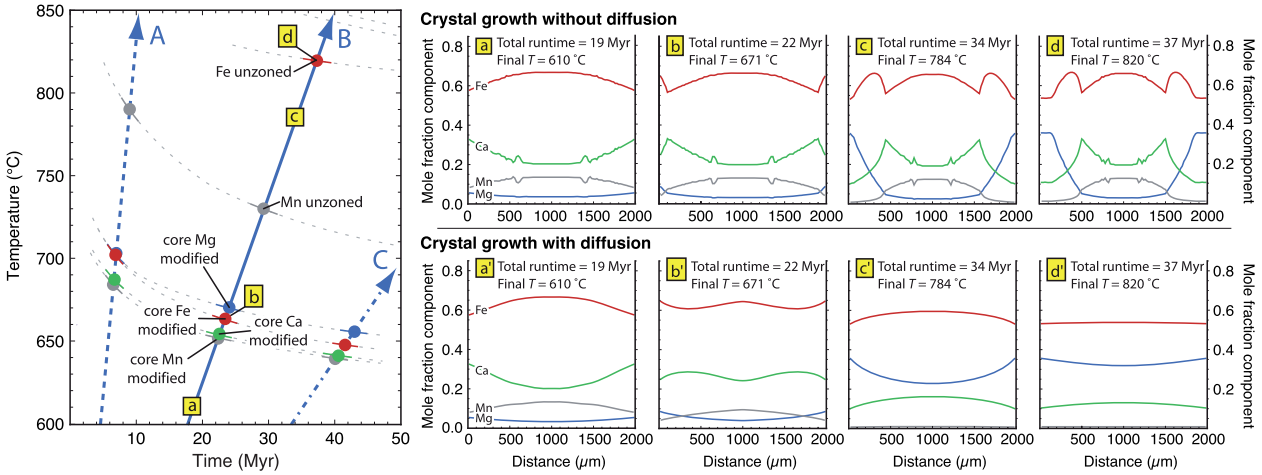

Fig. 5. Schematic representation of garnet profiles established during prograde *T*–*t* path B. Continuous (blue) line in left panel shows the heating path discussed in the text, with (yellow) labels ***a–d*** referring to points for which a growth profile is presented (panels at top right labelled ***a–d***). In each of panels ***a–d*** a rim–core–rim growth profile (without considering diffusion during heating) is shown through a modelled crystal that grew to 2 mm diameter in the interval from the garnet-in reaction to the temperature labelled. Panels ***a′–d′*** (bottom right) represent the same *T*–*t* histories as ***a–d*** (upper right), but with intra-crystalline diffusion calculated throughout the heating history. Coloured circles (left panel) reflect specific *T*–*t* conditions beyond which any crystal growing to 2 mm diameter will have appreciably modified core compositions or becomes unzoned (see text for details). Prograde paths A and C (left panel) show faster and slower heating rates, respectively, with displacement of the coloured circles representing core compositional modification to higher and lower temperature, accordingly (as discussed in the text).

Calculation of prograde metamorphic garnet growth zoning

Orogenic *P*–*T* histories generally involve garnet growth upon heating, or burial along a geotherm, and can involve partial resorption during cooling or exhumation. Although pre-existing crystals may survive entire orogenic events, even these cases may entail overgrowth (e.g. Argles *et al.*, 1999). The formation of chemical zoning invariably accompanies crystal growth (e.g. Hollister, 1966). Very short-duration metamorphic events may occasionally preserve clear petrographic evidence of 'chemical steps' in parts of garnet crystals that have been partially smoothed by diffusion and whose shape can be exploited to derive the diffusive duration (e.g. O'Brien, 1997; Dachs & Proyer, 2002; Ague & Baxter, 2007). Such information becomes lost over longer timescales, in which case growth zoning must be independently deduced before the effects of diffusional resetting can be examined.

Equilibrium phase stabilities as a function of *P* and *T* were calculated for two bulk-rock compositions (Appendix II). An average pelite and a natural granodiorite were chosen for illustration because they experience metamorphic garnet growth over a large *P*–*T* range, featuring a series of discrete pseudo-univariant reactions over this interval. As discussed further below and explored in detail by Konrad-Schmolke *et al.* (2006, 2007), identification of zoning discontinuities formed by garnet growth across these reactions can have important implications for the correct interpretation of mono- or poly-phase metamorphism. Garnet modal proportion and composition were calculated along prescribed burial and heating paths (from 400°C for the granodiorite, from 450°C for the pelite, up to a maximum of 850°C during burial to 50 km in both cases). These provided growth-zoning constraints (e.g. Fig. 5) under the assumption of rapid equilibration of the crystal rim and matrix (Appendix II). Figures 6a, b and 7a, b show that in both example rocks, garnet experiences a protracted growth history, despite the much smaller modal amount of garnet at P–T_{Max} in the meta-granodiorite than the meta-pelite.

The assumption of continual equilibration between a growing porphyroblast rim and the matrix implies that (1) no appreciable delay is associated with processes at the interface and (2) intergranular diffusion is sufficiently fast to retain an effectively homogeneous matrix. Modelled reaction rates support this, suggesting that local equilibrium between grains will be maintained for regional metamorphic heating rates, particularly as most prograde reactions liberate fluid which facilitates approach to chemical equilibrium (Walther & Wood, 1984). Here, the term 'matrix' implies a homogeneous mixture of all phases that constitute the rock but are not garnet, and without consideration of chemical heterogeneities arising from porphyroblasts of other minerals. Intra-crystalline zoning in this case is theoretically interpretable through changes in pressure, temperature or bulk-rock composition with time (e.g. Spear & Selverstone, 1983), with partitioning between the external 'reservoir' and the growing crystal considered

to be governed only by thermodynamically predictable coefficients.

Detailed studies of garnet crystal distributions and compositions further validate the assumption of hand-specimen-wide equilibration of most major components during garnet growth (with CaO being an exception; Chernoff & Carlson, 1997; Spear & Daniel, 2001). Significant disequilibrium has been suggested for rare earth element (REE) distribution during garnet growth (Chernoff & Carlson, 1999; Skora *et al.*, 2006), implying that equilibrium methods may not be suitable for trace elements. Recent work by Konrad-Schmolke *et al.* (2008), however, links complex REE zoning in garnet directly to discontinuous liberation through breakdown of a former host phase. New constraints on the thermodynamic properties of accessory minerals (e.g. Spear & Pyle, 2010) may be used to extend our approach by calculating trace element mineral budgets as a function of P and T.

Diffusional relaxation of chemical zoning during prograde garnet growth

Because our intention in this study is to predict the degree of intra-crystalline re-equilibration experienced before a crystal reaches T_{Max}, we modelled crystals undergoing a wide range of heating durations (1–50 Myr) to maximum temperatures in the range 500–850°C. Heating rates were constant during each calculation. The T range of garnet growth for both examined rock compositions is large, so slow heating rates allowed calculation of potentially significant re-equilibration of internal parts of the crystal before growth was completed. Multiple element diffusion was calculated with the cation diffusivity data of Carlson (2006) (Appendix I).

Four major parameters simultaneously control the zoning that will be present in a crystal at any point along a prograde P–T path: (1) the mineral reactions previously encountered and thus the chemical gradient established during growth; (2) the crystal size; (3) the temperature reached; (4) the duration spent reaching this temperature. Demonstration and discussion of the effects of these parameters requires objective criteria for assessing the zoning that is preserved in a crystal at the end of its heating history. This is clearly achieved by showing numerous radial-distance versus composition profiles (e.g. Florence & Spear, 1991; Gaidies *et al.*, 2008) that can then be classified into characteristic groups. However, this is less practical for demonstrating a large set of subtly different results and deconvolving the effects of the multiple parameters listed above, so we instead present a form of T–t plot with contours representing crystal sizes that experience specific amounts of diffusive homogenization. The logic behind this approach and the method we employed in its calculation are here described with reference to Fig. 5, where the blue T–t arrow (B) in the left panel represents an example P–T–t path (also shown by dashed dark grey line in P–T results, Fig. 6a). To simplify this introduction, we consider heating of the granodiorite because this encounters a less complicated set of pseudo-univariant mineral equilibria than the pelitic rock.

The prograde P–T–t path intercepts a garnet-in reaction (at lower temperature than 600°C in Fig. 5) and subsequently continues to adds rim overgrowths as temperature increases, subject to the successive mineral equilibria that it encounters. If the T–t path is truncated so that the maximum temperature attained is 610°C (point '***a***' on path B in the left panel of Fig. 5), crystal growth through the preceding multi-variant assemblage field will have established simple core-to-rim zoning. For a spherical crystal reaching a prescribed diameter of 2 mm at 610°C, the zoning profile produced by growth alone is shown in panel ***a*** (in the top right set of panels), and the profile formed by coupled growth and intra-crystalline diffusion is shown in panel ***a***′ (bottom right set of panels). Profiles ***a*** and ***a***′ are similar because the integrated diffusive history has been insufficient to significantly modify growth compositions (T was too low or t too short at this crystal size). Small-scale (*c.* 100 μm) steps in the growth profiles of Ca and Mn have, however, been diffusively relaxed.

Taking the same heating path as previously but instead truncating T_{Max} at 671°C (point '***b***' on T–t path B, Fig. 5) involves a major phase assemblage boundary [reaction (1), Fig. 6a]. The altered buffering assemblage causes subsequent garnet overgrowths to have distinctly different zoning trends in Fe, Mg, Ca and Mn. Profiles ***a*** and ***b*** (top right set of panels, Fig. 5) usefully highlight that a crystal growing to a diameter of 2 mm during heating to 671°C experiences identical equilibria to example ***a*** during its early history, here represented by zoning of the inner 1·76 mm of profile ***b***. The 3 Myr required to reach point ***b*** after ***a*** and the higher temperature experienced during this time are also sufficient for the effects of intra-crystalline diffusion to become pronounced, which is why profiles ***b*** and ***b***′ are distinctly different; ***b***′ broadly preserves the growth zoning trend, but not absolute compositions. Notably, at a specific time during heating to 671°C, diffusion first resulted in detectable modification of the initial growth content of Fe in the geometric crystal core. Ca and Mn contents have also been modified but the original growth content of Mg is effectively retained. Here we define 'detectable' as a 1% change from the initial growth composition, and mark the T–t at which this occurs with coloured circles for each element (Fig. 5, left panel).

A crystal growing to 2 mm diameter along an extension of the same P–T–t path to $T_{Max} = 784$°C develops far more complex zoning than previous examples if diffusion is not considered (profile ***c***, Fig. 5). It also experiences sufficient diffusive re-equilibration throughout this history to lose much of its original growth information (profile ***c***′).

In this case, detectable changes to the initial growth concentrations of all four considered cations in the crystal core occur well before T_{Max} is reached. Diffusion has also proceeded to such an extent that Mn is now effectively unzoned. The grey circle on heating path B at *c.* 730°C, 29·5 Ma (left panel of Fig. 5) records the conditions above which crystals reaching a final diameter of 2 mm would become un-zoned with respect to Mn, implying that this was the case for at least the final 4·5 Myr of growth in example ***c***′. General growth-zoning trends are preserved for all other components, but absolute compositions of the core (and indeed all parts of the crystal other than the outermost rim) have been lost. Crystal ***d***′ grows to 2 mm diameter in the interval from garnet-in to 820°C, retaining weak relict growth-zoning for only Mg and Ca, and very weak relict zoning for Fe (*c.* 1% X_{Gar}^{Fe} difference from core to rim).

Previous results (e.g. Jiang & Lasaga, 1990; Florence & Spear, 1991) show that the magnitude of compositional change through diffusion is highly dependent on heating rate, with faster heating permitting retention of initial core compositions to higher *T*. This is shown schematically by coloured circles on dashed and dash–dotted *T*–*t* paths A and C in Fig. 5, with an indication that contours could be constructed through each set of points if information were available for intermediate *T*–*t* paths. Similarly, if the growing crystal reaches less than 2 mm diameter at T_{Max} it is expected to preserve less zoning than larger crystals. To map out these relations in detail we repeatedly modelled crystal growth and diffusion during heating along a *P*–*T*–*t* path (e.g. blue *T*–*t* curve B in Fig. 5), truncating at each of 149 T_{Max} conditions along this path (rather than just the four conditions represented by profiles ***a***′, ***b***′, ***c***′ and ***d***′ in Fig. 5). These calculations were duplicated for crystals reaching prescribed maximum diameters of 500 μm, 1 mm, 1·5 mm, 2 mm, 3 mm, 5 mm and 1 cm. The entire process was then repeated for different *T*–*t* heating paths, exploring total heating durations in the range 1–50 Myr (equivalent to heating rates of <8°C Myr^{-1} to *c.* 450°C Myr^{-1}). The resultant matrix of *c.* 13 000 modelled crystal zoning profiles was examined and outputs were grouped according to (1) which crystal cores retained their initial compositions until the end of the simulation, (2) which cores had been partially modified following growth, and (3) which profiles had been modified to the point of effectively becoming unzoned crystals (classification criteria are outlined in more detail in Appendix III). Contours were calculated to represent crystals that satisfy these criteria in each of X_{Gar}^{Fe}, X_{Gar}^{Mg}, X_{Gar}^{Ca} and X_{Gar}^{Mn}, noting that although diffusion of all components is coupled, final zoning profiles are a function of both absolute D_{cation} values and the initial chemical gradients established during growth. Hence it is illustrative to independently calculate *T*–*t* plots for each element.

RESULTS

The prograde opening of crystals to diffusive modification of growth zoning

Continuous-line contours in Figs 6c–f and 7c–f represent garnet crystal diameters for which the crystal core composition at T_{Max} is exactly 0·01 mole-fraction units (1%) different (in either direction) from its initial prograde growth value. Larger crystals remain effectively unmodified from their growth composition (within the typical resolution of electron microprobe analysis), and smaller crystals experience a greater extent of compositional change (>0·01 mole-fraction units difference from the initial growth composition). All changes in crystal core composition result from addition of successive zoned overgrowths and subsequent cation diffusion upon heating. The *T*–*t* contours in Figs 6c–f and 7c–f have a similar form to those shown in Fig. 2, although now the axes show T_{Max} versus the time taken to reach that temperature at a constant heating rate (rather than the time spent at a static temperature, as in Fig. 2). This is a subtle but important distinction because any point within the *T*–*t* space of Figs 6 and 7 accounts for the integrated prograde growth and diffusion history (with associated changes in the equilibrium garnet composition) along the pre-T_{Max} burial path.

Stated simply, the contour sets in Figs 6c–f and 7c–f predict when longer duration or higher temperature events will begin to reset the core compositions of crystals of any particular grain size. For example, contours show that after 10 Myr of heating from 400 to 700°C, large (e.g. 1 cm diameter) crystals in the granodioritic rock effectively retain growth compositions in their cores but smaller crystals (e.g. 2 mm diameter) partially reset core contents of all four studied components (Fig. 6c–f, grey path 'b'). Heating to the same temperature but in just 1 Myr (Fig. 6c–f, grey path 'a') results in the effective retention of core growth compositions in all crystals larger than *c.* 1·5 mm diameter. Longer heating timescales (e.g. 50 Myr, Fig. 6c–f, path 'c') modify core compositions of larger crystals, although this size increase becomes less pronounced towards longer timescales as the contour slopes become shallow in *T*–*t* space.

Results for the pelitic rock (Fig. 7) are similar to those for the granodiorite (Fig. 6), but contours are displaced because core compositions of all components effectively begin to re-equilibrate earlier. This is partly due to the far higher initial X_{Gar}^{Ca} in the core of the pelitic garnet (compare Figs 6b and 7b), which increases the calculated diffusivity at any given *T* (Appendix I). D_{cation} values for the initial granodioritic and pelitic garnet core compositions, calculated with the data of Carlson (2006), differ by *c.* 2·5 orders of magnitude at any temperature (Appendix I, Fig. 8). Additionally, the chemical gradient ($\Delta X/l$) established during the early stages of the pelite garnet growth

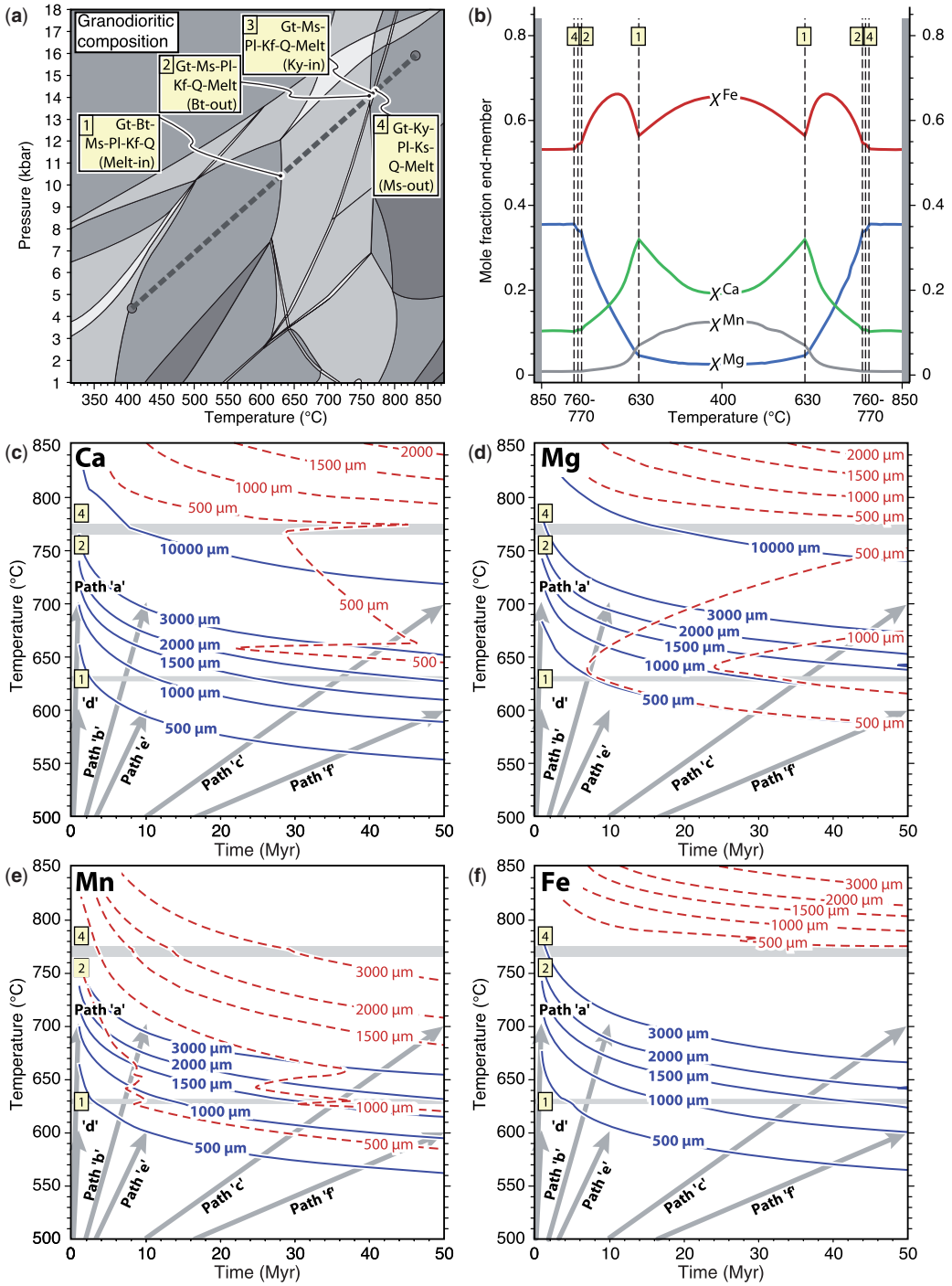

Fig. 6. Contoured results of modeled zoned garnet growth and diffusion during burial and heating of a granodioritic rock composition (Bohemian massif, sample KA-45b, Hradecký *et al.*, 2000) from 400°C, 4·5 kbar. (a) *P*–*T* pseudosection showing equilibrium mineral assemblages in this bulk-rock composition. Assemblage boundaries along model *P*–*T* path (bold dashed line) are numbered 1–4 and labelled with the stable phases plus the change (phase-in or phase-out) upon heating. Other assemblage labels have been removed for clarity (available as Supplementary Data). It should be noted that the diagram is calculated for a fixed bulk-rock composition and would not be fully valid if mass was fractionated from the bulk into growing porphyroblasts along any specific *P*–*T* path. (b) Profile through the core of a spherical garnet crystal showing the chemical zoning developed during heating to 850°C if diffusional relaxation does not occur. Zoning discontinuities form at assemblage boundaries [numbers 1–4 as in panel (a)]. Model crystals grow from a central core, so the *x*-axis (radial distance) equates to temperature of growth. (c) Plot of T_{Max} reached during heating and the time required to achieve that temperature at a constant heating rate. Contours (continuous lines with bold labels in micrometres) show crystal diameters below which final core Ca (grossular) content is diffusionally modified from its initial growth value (see Appendix III, and discussion of calculation method in text). Contours represent the final diameter achieved at T_{Max} and t_{total}. Dashed contours with labels in micrometres denote diameters of crystals that are effectively unzoned with respect to Ca (grossular) at the end of the simulation. Horizontal grey stripes represent discontinuities at mineral reactions (1)–(4) [as in (a) and (b)]. Grey arrows (labelled paths a–f) represent possible heating paths to 600 or 700°C in 1, 10 or 50 Myr, as a result of rapid or slow orogenic events (as in Fig. 1). (d–f) T_{Max}–t_{total} plot as (c) but showing contours for re-equilibration of Mg-pyrope (d), Mn-spessartine (e) and Fe-almandine (f) contents.

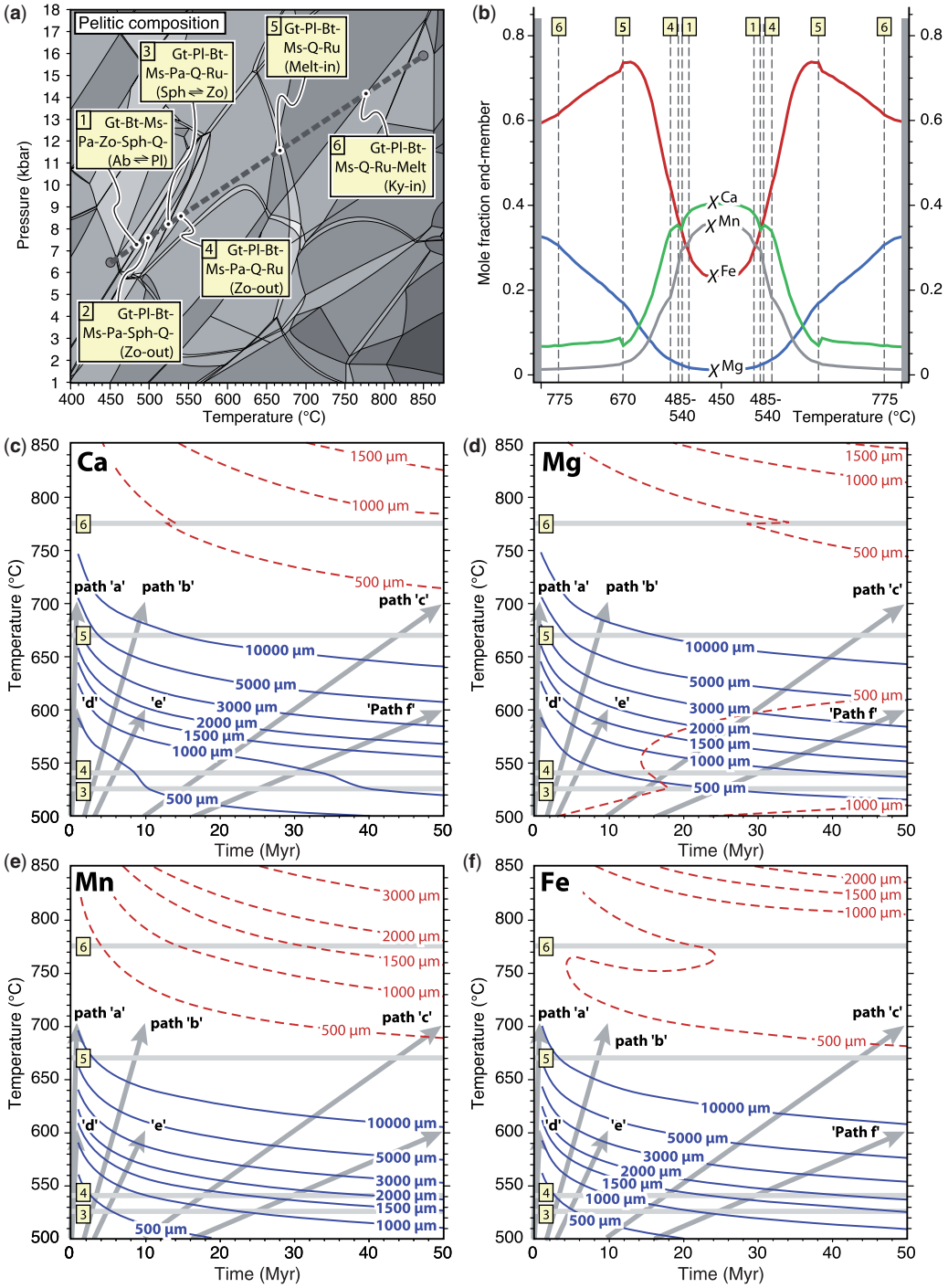

Fig. 7. As Fig. 6, but for an average pelitic rock composition (after Caddick & Thompson, 2008). (a) P–T pseudosection showing model heating path (bold dashed line) and labelled for key mineral reactions [numbers 1–6, labelled with stable assemblage plus the phase change (phase-in, phase-out or phases exchanged in parentheses) upon heating]. Fully labelled diagram available as Supplementary Data. (b) Profile through the core of a model garnet crystal grown during heating to 850°C but experiencing no volume diffusion. (c) T_{Max}–t_{total} plot contoured for diameter (micrometres) below which crystals have final core Ca (grossular) contents that are diffusionally modified from their initial growth value (continuous lines with bold labels) and diameters below which the final crystal is effectively unzoned with respect to grossular (dashed contours). Horizontal grey stripes denote numbered phase boundaries from (a) and (b). Grey arrows represent example heating paths, as in Fig. 6. (d–f) T_{Max}–t_{total} plots as in (c) but showing contours for re-equilibration of Mg, Mn and Fe contents, respectively.

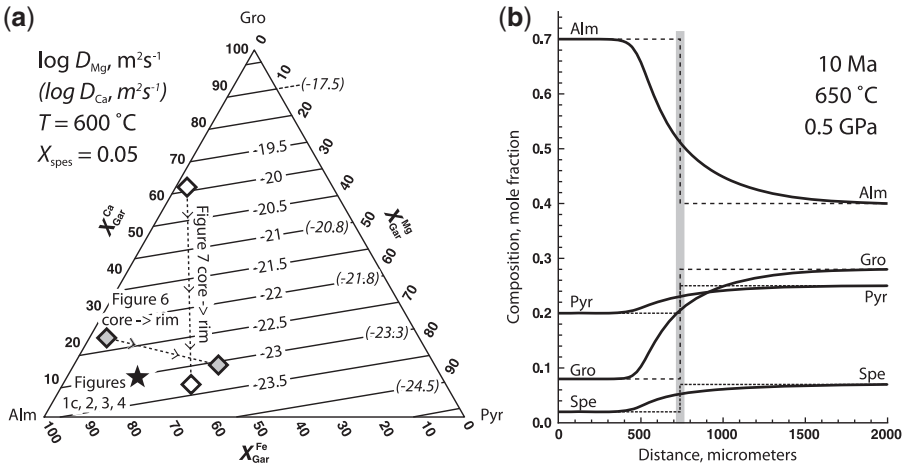

Fig. 8. (a) Mg tracer diffusivity (contours of $\log_{10}D_{Mg}$) plotted as a function of garnet composition (at 600°C, 1 GPa, graphite–oxygen) for a crystal with 5% spessartine [diffusion data after Carlson (2006)]. Approximate $\log_{10}D_{Ca}$ values also given in parentheses. Composition of Figs 1c, 2, 3 and 4 denoted with black star. Core and rim compositions of Figs 6b and 7b denoted by grey and white diamonds, respectively (arrows on tie lines point to rim composition). (b) Strongly asymmetric zoning profile (bold curves) resulting from diffusion across an initially stepped profile (dashed lines). Calculated for 10 Myr at 650°C with compositionally dependent D values and a planar geometry.

is far greater than for the granodiorite garnet (Figs 7b and 6b, respectively), again promoting more rapid re-equilibration of the former. It should be noted that for any t_{total}, core re-equilibration of a given crystal size effectively begins in paths reaching *c.* 75°C lower T_{Max} in the pelite calculations than for the granodiorite.

At low temperature, contours for the effective start of Ca re-equilibration in the cores of 500 and 1000 μm diameter pelitic garnet crystals (continuous lines, Fig. 7c) show additional complexities, revealing behaviour that cannot be easily explored with the analytical solutions. Contour inflections coincide with specific mineral reactions (numbered in Fig. 7a and b), such as at 525°C where a noticeable deceleration of core re-equilibration rate follows a sphene–zoisite reaction [numbered reaction (3)]. This itself follows a small field of increasingly X^{Ca}_{Gar}-rich overgrowth between assemblage boundaries 2 (*c.* 500°C) and 3 (525°C, see Fig. 7a and b), which lowers ΔX^{Ca}_{Gar} between the crystal core and rim and temporarily retards diffusive change of the core composition. Continued crystal growth with strongly decreasing X^{Ca}_{Gar} after zoisite-out [reaction (4) at *c.* 540°C] then increases core equilibration rate. Contour sets for components experiencing continual increase in abundance over the same T range (e.g. X^{Mg}_{Gar}, Fig. 7b) do not show similar inflexions (continuous lines, Fig. 7d).

Effective timescales for complete homogenization of previously zoned crystals

Dashed contours in Figs 6c–f and 7c–f show the T_{Max}–$t_{heating}$ relations at which modeled garnet crystals effectively preserve no growth zoning; that is, where any initial chemical gradient has been lost by diffusion. These reveal, for instance, that crystals reaching 500 μm diameter during 30 Myr heating to 800°C would be effectively unzoned in all elements at T_{Max}, but crystals growing to 1 mm diameter would retain slight zoning (in both examined rock compositions). Here we define 'slight zoning' as a difference in the mole-fraction of any element between core and rim of 0·01 (1%) or greater, which was chosen as a resolvable core–rim gradient with an electron microprobe. With this criterion a chemically homogeneous natural crystal can arise from a combination of (1) intra-crystalline diffusion during a long duration at high temperature, (2) multiple phases of growth with reversed zoning polarity, and (3) an absence of zoning established during growth (e.g. as a result of protracted buffering by an externally derived fluid, or by growth across a high-variance P–T interval featuring widely spaced compositional isopleths). The case of multiple overgrowths is well demonstrated by Fig. 6b, where the initial growth of garnet in the granodiorite [before reaction (1)] involves increasing X^{Ca}_{Gar} towards the crystal rim, but overgrowth after reaction (1) involves decreasing X^{Ca}_{Gar}. This second trend initially reduces the compositional difference between core and rim, reducing the time required for diffusive flattening of the zoning profile and shallowing the slope of the dashed 500 μm contour at *c.* 650°C (Fig. 6c). Continued overgrowth, with sustained decrease in X^{Ca}_{Gar}, eventually increases ΔX^{Ca}_{Gar} between core and rim (Fig. 6b). This increases the time required for diffusion to reduce ΔX^{Ca}_{Gar} towards 0·01, steepening the 500 μm contour until reaction (2) (biotite-out) at *c.* 770°C. X^{Mg}_{Gar} behaves differently over the same interval: a sharply

zoned overgrowth following reaction (1) dramatically and continuously increases ΔX_{Gar}^{Mg} between core and rim, retarding or effectively halting diffusive whole-crystal flattening. This is shown by overturned 500 μm and 1 mm contours in Fig. 6d, indicating that for both crystal sizes diffusive re-equilibration over this interval is slower than the addition of new material at the crystal rim for all but the slowest heating rates. Overgrowths following reaction (4) in the granodiorite (muscovite-out at $T = 770°C$, Fig. 6a and b) are effectively isochemical, so contours for loss of zoning of all components revert to a geometry typical for diffusion-driven relaxation of core to rim gradients.

Unlike contours for the effective opening of crystal cores to resetting, which typically occur at lower T or shorter timescales in pelitic than granodioritic garnet (continuous lines in Figs 6c–f and 7c–f, discussed above), contours representing complete flattening of zoning profiles occur later or at higher T in the pelitic calculations. This chiefly reflects the far larger chemical gradients established during growth of the pelitic garnet crystals (Fig. 7b), so that although noticeable re-equilibration begins earlier, more material must be diffused to yield a completely unzoned crystal. The result is a significantly larger T–t window between the beginning of re-equilibration and its effective conclusion in the pelitic case. P–T paths entering the staurolite field will feature a reduction in the size of this 'intermediate' T–t window, as partial garnet dissolution upon staurolite growth (Florence & Spear, 1993) and subsequent overgrowths with lower X_{Gar}^{Fe} reduce the total core-to-rim X_{Gar}^{Fe} gradient.

DISCUSSION

Mathematical methods (analytical and numerical) show simple relationships between the time at which the geometric core of a spherical garnet crystal will first be modified from its growth composition, the size of that crystal, and metamorphic temperature. Numerical results show how this time delay is also dependent on the magnitude and complexity of chemical gradients established during crystal growth and on the T–t history experienced (rather than simply T_{Max}). Furthermore, absolute initial crystal composition controls equilibration rates if diffusivities are considered to be composition dependent (e.g. Loomis *et al.*, 1985; Carlson, 2006). Exact resetting timescales are thus specific to a particular bulk-rock composition and P–T–t history, but the contour sets shown in Figs 6 and 7 suggest several important general trends that, because they span a large crystal composition range, may be considered as approximate end-members describing garnet zoning evolution rates.

An initial observation is that the effective temperature for opening of crystal cores to diffusional re-equilibration in the two examined bulk-rock compositions can differ by more than 100°C along any given heating path. For example, the core X_{Gar}^{Mg} of an eventual 1 mm diameter crystal undergoing burial and heating in the pelitic rock at 25°C Myr^{-1} (e.g. path 'b', Fig. 7d) will be modified from its growth composition if $T_{Max} > 580°C$ (*c.* 6 Myr of burial), shown by the intersection of path 'b' with the continuous-line 1 mm contour in Fig. 7d. A similar heating rate for the granodiorite retains the crystal core growth X_{Gar}^{Mg} content for T_{Max} up to 660°C (*c.* 8 Myr of burial, Fig. 6d). This disparity results from differences in diffusivity owing to the composition-dependent diffusion parameters used (Appendix I) and differences in the compositional gradients established during growth (reflecting the reactions responsible for garnet growth in the two rocks). Major phases of growth occur at different parts of the P–T path for each rock composition, such that crystals eventually reaching the same size at T_{Max} have different radii for most of the heating history. However, despite differences in the bulk-rock compositions, Figs 6 and 7 both suggest that almost all P–T paths involving heating to 700°C result in partial re-equilibration of the cores of millimetre-diameter crystals. The core compositions of larger (2–3 mm diameter) crystals will also be partially reset unless heating rate is very fast (250°C Myr^{-1} in the case of path 'a', Figs 6 and 7).

These factors also lead our pelitic results to differ from those of several previous studies, particularly indicating that more rapid heating to peak T is required to retain unmodified growth zoning for any crystal size. For example, Florence & Spear (1991) suggested that 4 mm or larger diameter crystals are required to preserve unmodified zoning if T reached 620°C during a 20–30 Myr metamorphic history, or if T reached 600°C during a 50 Myr history. This is broadly consistent with our results for Ca and Mg (Fig. 7c and d). We calculate, however, that Mn and Fe preserve growth compositions only in larger crystals (*c.* 1 cm diameter) for these T–t histories. Similarly, Florence & Spear (1991) recommended caution when interpreting P–T histories based on compositions of 1 mm diameter crystals that may have experienced temperatures greater than 560°C for durations of 40 Myr. Our results for all elements (Fig. 7c–f) suggest that growth compositions of the crystal core are lost earlier than this (<20 Myr of heating), although outer parts of the crystal change composition at a different rate. The main differences that lead to the shorter durations derived here are that larger chemical gradients are established during protracted garnet growth through multiple assemblage fields in our model, and that the criteria used here to distinguish diffusive modification are very sensitive to initial changes of the core composition. Furthermore, we used the diffusivity dataset of Carlson (2006), whereas Florence & Spear (1991) used the data of Loomis *et al.* (1985) with D_{Ca} assumed to be 0·5 D_{Fe}.

Importantly for mineral compositional thermobarometry, effective opening to resetting is different for each cation, reflecting differences in both tracer diffusivities and the compositional gradients established during growth. Consequently, crystal cores in modelled granodioritic garnets retain their growth X_{Gar}^{Mg} and X_{Gar}^{Fe} contents for longer than their X_{Gar}^{Mn} and X_{Gar}^{Ca} contents (e.g. path 'b' in Fig. 6 intersects the 3 mm diameter contour for X_{Gar}^{Mn} and X_{Gar}^{Ca} but only the 2 mm contour for X_{Gar}^{Mg} and X_{Gar}^{Fe}). In contrast, modelled pelitic garnets retain initial core X_{Gar}^{Ca} and X_{Gar}^{Mg} contents far later into the heating history than X_{Gar}^{Mn} and X_{Gar}^{Fe} (Fig. 7), although all components are modified by 600°C for most crystal sizes and heating rates. A simple implication of this is that X_{Gar}^{Ca} based geobarometry is unlikely to accurately reflect pressures of growth in many regional metamorphic cases, and should be applied with extreme caution to porphyroblasts and their inclusion assemblages unless there is additional evidence of a short thermal history.

Different timescales for effective opening to resetting of each element in any particular radial growth zone of a crystal illustrate how diffusion significantly modifies element ratios along the (core–rim) chemical profile. This emphasizes the need for careful selection of the most appropriate position within a crystal for multi-phase compositional thermobarometry. As shown in relation to Figs 2 and 3, and described elsewhere (e.g. Florence & Spear, 1991; Spear *et al.*, 1991; Gaidies *et al.*, 2008), the cores of large crystals are most appropriate for 'seeing further back' into a metamorphic history. Figure 7, however, cautions that even large (centimetre-scale) crystals that established zoning during growth will probably be subject to substantial compositional modification during heating to upper amphibolite-grade conditions. Indeed, Fig. 7 suggests that all pelitic garnets with final diameter ≤1 cm will experience detectable diffusional modification of their cores at $T_{Max} \geq 700$°C, unless the heating duration is less than *c.* 10 Myr. Cores of crystals with final diameter ≤2 mm (i.e. in the typical grain-size range of many natural schists and gneisses) are modified in the same duration at T_{Max} as low as 600°C. This supports early suggestions of a 'change-in-zoning-pattern isograd' (e.g. Yardley, 1977) and has significant implications for the reconstruction of complex P–T paths from natural samples. In the best case, reconstruction of P and T from partially relaxed growth zoning yields an apparent path that is shorter than the actual path experienced (i.e. the crystal zoning provides evidence only of its lattermost P–T history). In the worst case, because the rate of change of Ca:Mg:Fe:Mn ratios at any point within a crystal are different (although not independent of each other), P and T inferred from partially relaxed growth zoning may substantially depart from that experienced [as shown schematically by Spear *et al.* (1991), and for specific P–T paths by Florence & Spear (1991)]. Thus Figs 6 and 7 are most useful for determining the garnet crystal sizes most suitable for prograde P–T path reconstruction as T_{Max} is reached. 'Rapid' cooling is then also required to avoid further zoning modification and yield samples that are 'safe' for P–T path reconstruction by porphyroblast and mineral inclusion thermobarometry (by X_{Garnet} isopleth intersections in P–T pseudosections, or by the Gibbs method of differential thermodynamics).

Sensitivity of results to choice of diffusivity data

The work presented here is based upon calculations using the diffusivity data of Carlson (2006). A full description of the differences between this and other diffusivity datasets is not the aim of this contribution, but it is important to note how the resetting timescales derived here would be different (generally longer) with other data. Differences in the temperature dependence and pre-exponential constants of these datasets typically yield up to two orders of magnitude range between the fastest and slowest estimate of D^* for each element at any temperature between 400 to 900°C [an Arrhenius plot of diffusivity data from four groups of studies is available as Supplementary Data (Supplementary Fig. 4a)]. Two main reasons for this spread are that (1) most available laboratory experiments are at far higher temperature (generally >1100°C) than typical for metamorphism, so a large temperature extrapolation is required, and (2) experiments were conducted on a wide range of garnet compositions, so they should not all be directly comparable if diffusivity is dependent on garnet composition (Ganguly *et al.*, 1998).

With these aspects in mind, we used the data of Carlson (2006), which include low-temperature calibration points from stranded natural diffusion profiles (the coldest being 580°C) and resolve conflict between multiple experimentally derived datasets by normalizing data for crystal composition. Although uncertainties on both the D and T values retrieved for these natural samples are in all probability often higher than for each experimental datum, we feel that this additional regression 'anchor' at amphibolite-grade conditions permits more robust calculation at the wide range of temperatures that we are interested in here. We also note here that although the Carlson (2006) dataset yields faster low-T diffusion coefficients than previous calibrations for the garnet composition examined in Figs 1–4 (Supplementary Data Fig. 4a), the D^* values calculated for likely 'early' (Mn and Ca-rich) and 'late' (Mg-rich) garnet growth compositions encompass the range of most of these other datasets. The Ca diffusivity data of Vielzeuf *et al.* (2007) fall within this range at temperatures below 700°C, predicting slower D_{Ca}^* than the Carlson (2006) data as temperature increases.

T–t window for the onset and culmination of relaxation of garnet zoning

Recognition of specific zoning patterns that yield the most readily interpretable *P–T* information requires chemical analysis at high spatial resolution, but has considerable additional value when using diffusion-modified chemical profiles to retrieve time information (i.e. geospeedometry, Lasaga, 1983). It is evident from Figs 6 and 7 that a very broad *T–t* window exists between the onset of effective whole-crystal re-equilibration (continuous-line curves) and complete crystal homogenization (dashed-line curves). Within this region millimetre-scale crystals retain evidence for growth zoning up to relatively high temperature, but the absolute compositions preserved can be significantly different from original growth values. It is important to note that there might be little independent evidence to demonstrate that the growth zoning preserved in such crystals does not in fact record absolute compositions during growth. The cores of small garnet crystals ($<$500 μm) are first modified at very low temperatures ($<$550°C) unless heating is 'rapid', but some evidence of prograde zoning can be retained for significantly longer ($T_{Max} > 750$°C). In general, the larger the compositional gradients established during growth (i.e. the larger the range of *P–T* conditions over which growth occurs, or the greater the amount of fractionation from the rock during growth), the larger will be the resultant *T–t* window between the 'onset' and 'completion' of intra-crystalline zoning relaxation.

Implications for the rates of tectonic processes

Methods for discerning the duration of prograde metamorphism help in deducing the depth and longevity of heat sources for specific tectonic episodes, and can be coupled with thermo-tectonic models for subsequent exhumation mechanisms. In particular, the retention of short length-scale disequilibrium features in medium- and high-grade rocks is a sensitive record of rapid ($\ll$1 to 10 Myr) thermal events. Such characteristic heating rates during metamorphism are indicative of specific heat sources and/or displacement mechanisms (Fig. 1d), with approximate limits set by the characteristic heat conduction length (e.g. *c.* 1 cm a^{-1}, Lachenbruch *et al.*, 1976) and average plate-tectonic velocities (*c.* 1 to $>$5 cm a^{-1}). More rapid orogenic and thermal development would require special tectonic geometries (such as channelized extrusion, e.g. Thompson *et al.*, 1997; Ellis *et al.*, 1998) or additional heat sources (such as shear heating, e.g. Molnar & England, 1990; Burg & Gerya, 2005). For example, the three rates for prograde Barrovian-type metamorphism shown in Fig. 1d would require varying combinations of radiogenic heating with conduction, advection with internal shear heating, or advection by melt or fluid. Determination of metamorphic timescale typically requires either analysis of a suite of isotopically datable phases or preservation of 'partially diffused' compositional steps from which diffusion modelling can proceed. Forward modelling of garnet growth zoning, however, permits independent constraint of the 'pre-diffusion' cation configuration, potentially increasing the utility of geospeedometry to recover a larger range of metamorphic timescales than previously possible.

CONCLUSIONS

Even acknowledging that all exposed metamorphic garnets might have undergone a lengthy exhumation history and therefore additional diffusional resetting during cooling, the present study emphasizes which aspects of zoning profiles could have been modified even during the prograde heating history. This provides simple methods to determine which garnet core compositions are likely to remain unmodified by prograde diffusion and which are likely to have experienced significant flattening of chemical gradients.

Rapid exhumation histories can preserve relict core compositions in garnet crystals if they experience minimal heating during exhumation (e.g. during extrusion; see fig. 4 of Thompson *et al.*, 1997). Thus to preserve initial core compositions up to T_{Max} and have any realistic possibility of deducing early *P–T* conditions by simple geo-thermobarometry, pelitic garnet crystals experiencing amphibolite-grade conditions should be at least 5 mm in diameter unless there is evidence that metamorphism was fast (less than *c.* 10 Myr). These sizes substantially increase (several centimetres) when peak metamorphic temperatures enter the granulite-facies, where the likelihood of elimination of growth zoning long before exhumation begins is high. We emphasize again here the large gap along any *T–t* path between 'opening' of a crystal core to efficient diffusion (continuous-line contours, Figs 6 and 7) and advanced stages of diffusion which yield an effectively unzoned crystal (dashed-line contours, Figs 6 and 7). This favours the common preservation of *trends* of prograde elemental zoning, despite significant modification of original absolute growth compositions.

Interpretation of garnet zoning patterns in terms of the *T–t* history provides a useful prelude to geochemical methods directed at determining age variation and evaluating metamorphic duration (e.g. laser-ablation mass spectrometry on cores and rims of accessory phases, secondary ionization mass spectrometry, thermal ionization mass spectrometry on carefully selected and prepared garnet separates). Diffusion modelling of additional elements whose diffusivities lie outside the range considered here (*c.* 10^{-21}–10^{-27} m^2 s^{-1} at the temperatures of interest for most metamorphic processes) would allow extension of

the timescale to shorter intervals, but requires both calibration of additional species (e.g. REE diffusion in garnet) and high spatial resolution analyses of natural samples.

ACKNOWLEDGEMENTS

We particularly thank M. Konrad-Schmolke and C. Foster for especially constructive criticism during review, and R. Gieré for considerate editorial handling. We thank an anonymous reviewer, M. Kohn and F. Spear for valuable comments on an earlier version of this paper.

FUNDING

This project was supported by ETH Research Funds to M.J.C. and A.B.T. J.K. appreciates the support of the Czech Republic Ministry of Education, Youth & Sports, through the Scientific Centre 'Advanced Remedial Technologies and Processes' (I.D. code 1M0554).

SUPPLEMENTARY DATA

Supplementary data for this paper are available at *Journal of Petrology* online.

REFERENCES

Ague, J. J. & Baxter, E. F. (2007). Brief thermal pulses during mountain building recorded by Sr diffusion in apatite and multicomponent diffusion in garnet. *Earth and Planetary Science Letters* **261**, 500–516.

Anderson, D. E. & Olimpio, J. C. (1977). Progressive homogenization of metamorphic garnets, south Morar, Scotland: Evidence for volume diffusion. *Canadian Mineralogist* **15**, 205–216.

Argles, T. W., Prince, C. I., Foster, G. L. & Vance, D. (1999). New garnets for old? Cautionary tales from young mountain belts. *Earth and Planetary Science Letters* **172**, 301–309.

Burg, J. P. & Gerya, T. V. (2005). The role of viscous heating in Barrovian metamorphism of collisional orogens: thermomechanical models and application to the Lepontine Dome in the Central Alps. *Journal of Metamorphic Geology* **23**, 75–95.

Caddick, M. J. & Thompson, A. B. (2008). Quantifying the tectono-metamorphic evolution of pelitic rocks from a wide range of tectonic settings: Mineral compositions in equilibrium. *Contributions to Mineralogy and Petrology* **156**, 177–195.

Camacho, A., Lee, J. K. W., Hensen, B. J. & Braun, J. (2005). Short-lived orogenic cycles and the eclogitization of cold crust by spasmodic hot fluids. *Nature* **435**, 1191–1196.

Carlson, W. D. (1989). The significance of intergranular diffusion to the mechanisms and kinetics of porphyroblast crystallization. *Contributions to Mineralogy and Petrology* **103**, 1–24.

Carlson, W. D. (2006). Rates of Fe, Mg, Mn and Ca diffusion in garnet. *American Mineralogist* **91**, 1–11.

Carslaw, H. S. & Jaeger, C. J. (1959). *Conduction of Heat in Solids*. Oxford: Clarendon.

Chakraborty, S. (2006). Diffusion modeling as a tool for constraining timescales of evolution of metamorphic rocks. *Mineralogy and Petrology* **88**, 7–27.

Chakraborty, S. & Ganguly, J. (1991). Compositional zoning and cation diffusion in garnets. In: Ganguly, J. (ed.) *Diffusion, Atomic Ordering, and Mass Transport*. New York: Springer, pp. 120–175.

Cherniak, D. J., Watson, E. B., Grove, M. & Harrison, T. M. (2004). Pb diffusion in monazite: A combined RBS/SIMS study. *Geochimica et Cosmochimica Acta* **68**, 829–840.

Chernoff, C. B. & Carlson, W. D. (1997). Disequilibrium for Ca during growth of pelitic garnet. *Journal of Metamorphic Geology* **15**, 421–438.

Chernoff, C. B. & Carlson, W. D. (1999). Trace element zoning as a record of chemical disequilibrium during garnet growth. *Geology* **27**, 555–558.

Christensen, J. N., Selverstone, J., Rosenfeld, J. L. & De Paolo, D. J. (1994). Correlation by Rb–Sr geochronology of garnet growth histories from different structural levels within the Tauern Window, Eastern Alps. *Contributions to Mineralogy and Petrology* **118**, 1–12.

Connolly, J. A. D. (1990). Multivariable phase diagrams: an algorithm based on generalized thermodynamics. *American Journal of Science* **290**, 666–718.

Connolly, J. A. D. (2005). Computation of phase equilibria by linear programming: A tool for geodynamic modeling and its application to subduction zone decarbonation. *Earth and Planetary Science Letters* **236**, 524–541.

Crank, J. (1956). *The Mathematics of Diffusion*. London: Clarendon Press.

Crank, J. (1975). *The Mathematics of Diffusion*, 2nd edn. Oxford: Clarendon Press.

Dachs, E. & Proyer, A. (2002). Constraints on the duration of high-pressure metamorphism in the Tauern Window from diffusion modelling of discontinuous growth zones in eclogite garnet. *Journal of Metamorphic Geology* **20**, 769–780.

Darken, L. S. & Gurry, R. W. (1953). *Physical Chemistry of Metals*. New York: McGraw–Hill.

Dempster, T. J. (1985). Garnet zoning and metamorphism of the Barrovian Type area, Scotland. *Contributions to Mineralogy and Petrology* **89**, 30–38.

Dewey, J. F. (1997). Orogeny can be very short. *Proceedings of the National Academy of Sciences of the USA* **102**, 15286–15293.

Dewey, J. F. & Mange, M. (1999). Petrology of Ordovician and Silurian sediments in the Western Irish Caledonides: tracers of short-lived Ordovician continent–arc collision orogeny and the evolution of the Laurentian Appalachian–Caledonian margin. In: Mac Niocaill, C. & Ryan, P. D. O. (eds) *Continental Tectonics. Geological Society, London, Special Publications* **164**, 55–108.

Dodson, M. H. (1973). Closure temperature in cooling geochronological and petrological systems. *Contributions to Mineralogy and Petrology* **40**, 259–274.

Ellis, S., Beaumont, C., Jamieson, R. A. & Quinlan, G. (1998). Continental collision including a weak zone: the vise model and its application to the Newfoundland Appalachians. *Canadian Journal of Earth Sciences* **35**, 1323–1346.

Faryad, S. W. & Chakraborty, S. (2005). Duration of Eo-Alpine metamorphic events obtained from multicomponent diffusion modeling of garnet: a case study from the Eastern Alps. *Contributions to Mineralogy and Petrology* **150**, 306–318.

Florence, F. P. & Spear, F. S. (1991). Effects of diffusional modification of garnet growth zoning on P–T path calculations. *Contributions to Mineralogy and Petrology* **107**, 487–500.

Florence, F. P. & Spear, F. S. (1993). Influences of reaction history and chemical diffusion on P–T calculations for staurolite schists from the Littleton Formation, northwestern New Hampshire. *American Mineralogist* **78**, 345–359.

Foster, G. L., Parrish, R. R., Horstwood, M. S. A., Chenery, S., Pyle, J. M. & Gibson, H. D. (2004). The generation of prograde *P–T–t* points and paths; a textural, compositional, and chronological study of metamorphic monazite. *Earth and Planetary Science Letters* **228**, 125–142.

Gaidies, F., De Capitani, C. & Abart, R. (2008). THERIAG: a software program to numerically model prograde garnet growth. *Contributions to Mineralogy and Petrology* **155**, 657–671.

Ganguly, J., Chakraborty, S., Sharp, T. G. & Rumble, D. (1996). Constraint on the time scale of biotite-grade metamorphism during Acadian orogeny from a natural garnet–garnet diffusion couple. *American Mineralogist* **81**, 1208–1216.

Ganguly, J., Cheng, W. & Chakraborty, S. (1998). Cation diffusion in aluminosilicate garnets: experimental determination in pyrope–almandine diffusion couples. *Contributions to Mineralogy and Petrology* **131**, 171–180.

Ganguly, J., Dasgupta, S., Cheng, W. & Neogi, S. (2000). Exhumation history of a section of the Sikkim Himalayas, India: records in the metamorphic mineral equilibria and compositional zoning of garnet. *Earth and Planetary Science Letters* **183**, 471–486.

Harris, C. R., Hoisch, T. D. & Wells, M. L. (2007). Construction of a composite pressure–temperature path: revealing the synorogenic burial and exhumation history of the Sevier hinterland, USA. *Journal of Metamorphic Geology* **25**, 915–934.

Harrison, T. M., Grove, M., Lovera, O. M. & Catlos, E. J. (1998). A model for the origin of Himalayan anatexis and inverted metamorphism. *Journal of Geophysical Research* **103**, 27017–27032.

Holland, T. J. B. & Powell, R. (1998). An internally consistent thermodynamic data set for phases of petrological interest. *Journal of Metamorphic Geology* **16**, 309–343.

Hollister, L. S. (1966). Garnet zoning: an interpretation based on the Rayleigh fractionation model. *Science* **154**, 1647–1651.

Hradecký, P., Adamová, M., Bohdánek, P., Elznic, A., Godány, J., Hrazdíra, P., Kotková, J., Manová, M., Mlčoch, B., Nekovařík, Č., Šalanský, K. & Šebesta, J. (2000). Explanation to 1:25,000 geological map of the Czech Republic, sheet 11-222. Prague: Czech Geological Survey.

Inui, M. & Toriumi, M. (2002). Prograde pressure–temperature paths in the pelitic schists of the Sambagawa metamorphic belt, SW Japan. *Journal of Metamorphic Geology* **20**, 563–580.

Jiang, J. & Lasaga, A. C. (1990). The effect of post-growth thermal events on growth-zoned garnet: implications for metamorphic *P–T* history calculations. *Contributions to Mineralogy and Petrology* **105**, 454–459.

Kohn, M. J., Spear, F. S. & Valley, J. W. (1997). Dehydration-melting and fluid recycling during metamorphism: Rangeley Formations, New Hampshire, USA. *Journal of Petrology* **38**, 1255–1277.

Konrad-Schmolke, M., Babist, J., Handy, M. R. & O'Brien, P. J. (2006). The physico-chemical properties of a subducted slab from garnet zonation patterns (Sesia Zone, Western Alps). *Journal of Petrology* **47**, 2123–2148.

Konrad-Schmolke, M., O'Brien, P. J., De Capitani, C. & Carswell, D. A. (2007). Garnet growth at high- and ultra-high pressure conditions and the effect of element fractionation on mineral modes and composition. *Lithos* **103**, 309–332.

Konrad-Schmolke, M., Zack, T., O'Brien, P. J. & Jacob, D. E. (2008). Combined thermodynamic and rare earth element modelling of garnet growth during subduction: Examples from ultrahigh-pressure eclogite of the Western Gneiss Region, Norway. *Earth and Planetary Science Letters* **272**, 488–498.

Kretz, R. (1973). Kinetics of the crystallization of garnet at two localities near Yellowknife. *Canadian Mineralogist* **12**, 1–20.

Kretz, R. (1993). A garnet population in Yellowknife schist, Canada. *Journal of Metamorphic Geology* **11**, 101–120.

Lachenbruch, A. R., Sass, J. H., Munroe, R. J. & Moses, T. H. (1976). Geothermal setting and simple heat conduction models for the Long Valley caldera. *Journal of Geophysical Research* **81**, 769–784.

Lasaga, A. C. (1979). Multicomponent exchange and diffusion in silicates. *Geochimica et Cosmochimica Acta* **43**, 455–469.

Lasaga, A. C. (1983). Geospeedometry: An extension of geothermometry. In: Saxena, S. K. (ed.) *Kinetics and Equilibrium in Mineral Reactions*. New York: Springer, pp. 81–114.

Loomis, T. P., Ganguly, J. & Elphick, S. C. (1985). Experimental determination of cation diffusivities in aluminosilicate garnets II. Multicomponent simulation and tracer diffusion coefficients. *Contributions to Mineralogy and Petrology* **90**, 45–51.

Molnar, P. & England, P. C. (1990). Temperatures, heat flux, and frictional stress near major normal thrust faults. *Journal of Geophysical Research* **95**, 4833–4856.

O'Brien, P. J. (1997). Garnet zoning and reaction textures in overprinted eclogites, Bohemian Massif, European Variscides: A record of their thermal history during exhumation. *Lithos* **41**, 119–133.

O'Brien, P. J. & Vrana, S. (1995). Eclogites with a short-lived granulite facies overprint in the Moldanubian Zone, Czech Republic: Petrology, geochemistry and diffusion modelling of garnet zoning. *Geologische Rundschau* **84**, 473–488.

Oliver, G. J. H., Chen, F., Buchwaldt, R. & Hegner, E. (2000). Fast tectonometamorphism and exhumation in the type area of the Barrovian and Buchan zones. *Geology* **28**, 459–462.

Onsager, L. (1945). Theories and problems of liquid diffusion. *Annals of the New York Academy of Sciences* **46**, 241–265.

Perchuk, A. L. & Philippot, P. (1997). Rapid cooling and exhumation of eclogitic rocks from the Great Caucasus, Russia. *Journal of Metamorphic Geology* **15**, 299–310.

Reiners, P. W., Ehlers, T. A. & Zeitler, P. K. (2005). Past, present and future of thermochronology. In: Reiners, P. W. & Ehlers, T. A. (eds) *Low-temperature Thermochronology: Techniques, Interpretations and Applications*. Chantilly, VA: Mineralogical Society of America, pp. 1–18.

Rubatto, D. & Hermann, J. (2001). Exhumation as fast as subduction? *Geology* **29**, 3–6.

Skora, S., Baumgartner, L. P., Mahlen, N. J., Johnson, C. M., Pilet, S. & Hellebrand, E. (2006). Diffusion-limited REE uptake by eclogite garnets and its consequences for Lu–Hf and Sm–Nd geochronology. *Contributions to Mineralogy and Petrology* **152**, 703–720.

Spear, F. S. (1988). Metamorphic fractional crystallization and internal metasomatism by diffusional homogenization of zoned garnets. *Contributions to Mineralogy and Petrology* **99**, 507–517.

Spear, F. S. (1991). On the interpretation of peak metamorphic temperatures in light of garnet diffusion during cooling. *Journal of Metamorphic Geology* **9**, 379–388.

Spear, F. S. (1993). *Metamorphic Phase Equilibria and Pressure–Temperature–Time Paths*. Washington DC: Mineralogical Society of America.

Spear, F. S. & Daniel, C. G. (2001). Diffusion control of garnet growth, Harpswell Neck, Maine, USA. *Journal of Metamorphic Geology* **19**, 179–195.

Spear, F. S. & Florence, F. P. (1992). Thermobarometry in granulites: pitfalls and new approaches. *Precambrian Research* **55**, 209–241.

Spear, F. S. & Pyle, J. M. (2010). Theoretical modeling of monazite growth in a low-Ca metapelite. *Chemical Geology* **273**, 111–119.

Spear, F. S. & Selverstone, J. (1983). Quantitative *P–T* paths from zoned minerals: theory and tectonic applications. *Contributions to Mineralogy and Petrology* **83**, 348–357.

Spear, F. S., Kohn, M. J., Florence, F. P. & Menard, T. (1991). A model for garnet and plagioclase growth in pelitic schists: Implications for thermobarometry and P–T path determinations. *Journal of Metamorphic Geology* **8**, 683–696.

St-Onge, M. R. (1987). Zoned poikiloblasic garnets: P–T paths and syn-metamorphic uplift through 30 km of structural depth, Wopmay Orogen, Canada. *Journal of Petrology* **28**, 1–21.

Storm, L. C. & Spear, F. S. (2005). Pressure, temperature and cooling rates of granulite facies migmatitic pelites from the southern Adirondack Highlands, New York. *Journal of Metamorphic Geology* **23**, 107–130.

Stüwe, K. & Ehlers, K. (1996). The qualitative zoning record of minerals. A method for determining the duration of metamorphic events. *Mineralogy and Petrology* **56**, 171–184.

Thompson, A. B. & England, P. C. (1984). Pressure–temperature–time paths of regional metamorphism II. Their inference and interpretation using mineral assemblages in metamorphic rocks. *Journal of Petrology* **25**, 929–955.

Thompson, A. B., Schulmann, K. & Jezek, J. (1997). Thermal evolution and exhumation in obliquely convergent (transpressive) orogens. *Tectonophysics* **280**, 171–184.

Tracy, R. J., Robinson, P. & Thompson, A. B. (1976). Garnet composition and zoning in the determination of temperature and pressure of metamorphism, central Massachusetts. *American Mineralogist* **61**, 762–775.

Vance, D. & O'Nions, R. K. (1990). Isotopic chronometry of zoned garnets: growth kinetics and metamorphic histories. *Earth and Planetary Science Letters* **97**, 117–240.

Vielzeuf, D., Baronnet, A., Perchuk, A. L., Laporte, D. & Baker, M. B. (2007). Calcium diffusivity in alumino-silicate garnets: an experimental and ATEM study. *Contributions to Mineralogy and Petrology* **154**, 153–170.

Walther, J. V. & Wood, B. J. (1984). Rate and mechanism in prograde metamorphism. *Contributions to Mineralogy and Petrology* **79**, 252–257.

Watson, E. B. & Baxter, E. F. (2007). Diffusion in solid-Earth systems. *Earth and Planetary Science Letters* **253**, 307–327.

White, R. W., Powell, R. & Holland, T. J. B. (2007). Progress relating to calculation of partial melting equilibria for metapelites. *Journal of Metamorphic Geology* **25**, 511–527.

Woodsworth, G. J. (1977). Homogenization of zoned garnets from pelitic schists. *Canadian Mineralogist* **15**, 230–242.

Yardley, B. W. D. (1977). An empirical study of diffusion in garnet. *American Mineralogist* **62**, 793–800.

Zulauf, G., Dorr, W., Fiala, J., Kotkova, J., Maluski, H. & Valverde-Vaquero, P. (2002). Evidence for high-temperature diffusional creep preserved by rapid cooling of lower crust (North Bohemian shear zone, Czech Republic). *Terra Nova* **14**, 343–354.

APPENDIX I: MODEL OF P–T–X-DEPENDENT DIFFUSIVITY

Radial, multi-component diffusion in a sphere was calculated with an explicit finite-difference model using an expansion (Onsager, 1945) of Fick's second law for three independent (Fe, Mg, Mn) and one dependent (Ca) species (Crank, 1956):

$$\frac{\partial X}{\partial t} = \frac{1}{r^2}\frac{\partial}{\partial r}\left[r^2 D \frac{\partial X}{\partial r}\right] \tag{4}$$

in which X is a vector of mole-fraction terms, D is a matrix of interdependent diffusion coefficients and r is radius (as used in spherical or linear geometries by several recent studies; e.g. Florence & Spear, 1991; Spear, 1993; Dachs & Proyer, 2002; Gaidies *et al.*, 2008). The crystal rim composition was fixed, as determined by equilibrium thermodynamic calculations for each P and T. Δt was varied throughout each model run, with small time-steps maintaining numerical stability at large values of D. The D matrix was calculated at each time-step and crystal position using an expression for ionic solutions (Lasaga, 1979):

$$D_{ij} = D_i^* \delta_{ij} - \left[\frac{D_i^* X_i}{\sum_{k=1}^{4} D_k^* X_k}\right]\left(D_j^* - D_{\mathrm{Ca}}^*\right) \tag{5}$$

in which $D^*_{i,j,\mathrm{Ca}}$ are cation tracer diffusivities and δ_{ij} is Kronecker's delta. D^* values for Fe, Mg, Mn and Ca in both numerical and analytical calculations were a function of the intensive variables and composition (which is position and time dependent in the numerical model) following Carlson (2006):

$$\ln D_i^* = \ln D_{0,i}^* + \Delta\alpha_{0,i} - \frac{Q_i + P\Delta V_i}{RT} + \frac{1}{6}\ln\left(\frac{f_{\mathrm{O2}}}{f_{\mathrm{O2}}^{\mathrm{graphite}}}\right) \tag{6}$$

where Q_i and V_i are the molar activation energy and volume, respectively. $\Delta\alpha_{0,i}$ is the scaled product of the difference in unit cell size between end-member i and the crystal composition (following Carlson, 2006). Oxygen fugacity was fixed at graphite–oxygen equilibrium. The compositional dependence of D_i^* for crystal compositions discussed in this paper are shown in Fig. 8a. Figure 8b demonstrates a consequence of calculating the D-matrix from these data; namely, that strongly asymmetric zoning profiles can form upon diffusion across initially simple compositional steps. It should be noted, however, that this does not violate mass-balance constraints.

APPENDIX II: CONSTRAINING GROWTH ZONING

Gibbs free-energy minimization calculations used the Perple_X program of Connolly (1990, 2005), with end-member thermodynamic data from Holland & Powell (1998; dataset revision *tcds55*). We used the solid-solution models listed in table 2 of Caddick & Thompson (2008), with biotite and garnet modified after White *et al.* (2007). Crystal growth zoning was established by calculating the modal proportion (M_{Gar}) and equilibrium composition (X_{Gar}) of garnet and converting them into crystal radius and rim composition at successive points along a prescribed P–T path, assuming a spherical

crystal geometry. The reactive (bulk-rock) composition was not modified at this point to account for sequestration of chemical components into newly formed mineral grains. Changes in the 'effective bulk-composition' owing to porphyroblast growth and re-equilibration were described in detail by Spear (1988) and such (P–T-path specific) fractionation increases the initial chemical gradients established during growth (e.g. Hollister, 1966; Florence & Spear, 1991; Gaidies *et al.*, 2008), as quantified for a specific heating history in fig. 17-13 of Spear (1993). This is clearly important for accurately deducing the specific mineral reactions encountered during growth of any natural crystal (e.g. Konrad-Schmolke *et al.*, 2007) but we found it to have little effect on the crystal-scale equilibration timescales presented here (e.g. Figs 6c–f and 7c–f). These are controlled more strongly by the T dependence of D.

Because we are interested here in crystals that can preserve information about early prograde history, we concentrate specifically on crystals that nucleated immediately upon crossing the garnet-in reaction for an imposed P–T path; crystals nucleating later along the same path may record a subset of this information (Kretz, 1973, 1993; Carlson, 1989; Gaidies *et al.*, 2008), but we do not consider them here. Following Florence & Spear (1991), garnet nucleation density (and thus final crystal radius for a given volume proportion of garnet) was considered to be an independent variable. The desired final crystal radius (r_{Max}) was assigned to the P–T point where the highest M_{Gar} value intersected the P–T path, and preceding values of r during growth were scaled accordingly. Model crystals contained 101 positional nodes, with node spacing a function of r_{Max}. At each time-step, the composition of the outermost node was constrained by the equilibrium garnet composition at the relevant P–T condition along the P–T path.

APPENDIX III: CRYSTAL-RADIUS–TEMPERATURE–TIME CONTOURING

Two parameters were extracted from the matrix of model results to describe the limits of diffusional relaxation: (1) the time during heating at which a crystal core composition is first detectably altered from its growth value by diffusion; (2) the subsequent time at which the crystal first becomes effectively unzoned through diffusion. Changes in either the chemical gradient or absolute core composition could be tracked, but we are most interested in the preservation potential of measurable crystal compositions so we define $\Delta_t X_i = \left| X_i^{\text{initial-core}} - X_i^{\text{final-core}} \right|$ (the absolute change in abundance of component i in the crystal core during each simulation). $\Delta_t X_i \geq 0{\cdot}01$ (1%) was considered to represent crystals whose cores experienced partial re-equilibration during heating and $\Delta_t X_i < 0{\cdot}01$ to represent crystals whose cores maintained their original growth composition (1% was chosen to represent a small, but determinable quantity by electron microprobe). Final crystal zoning was defined with $\Delta_l X_i = \left| X_i^{\text{final-core}} - X_i^{\text{final-rim}} \right|$, representing the difference in composition of the crystal core and rim at the end of the simulation. $\Delta_l X_i \leq 0{\cdot}01$ represents effectively unzoned garnet crystals and $\Delta_l X_i > 0{\cdot}01$ represents crystals retaining some zoning. The array of *c.* 13 000 model outputs was contoured according to these criteria to illustrate T_{max}–t_{total}–l_{final} relationships at which diffusional re-equilibration begins to modify crystal cores and eventually results in unzoned crystals (Figs 6 and 7). This technique is similar to that described by Chakraborty & Ganguly (1991), but with the important distinctions that here the simulation is poly-thermal, the modelled crystal boundary moves as a function of time, and the cation diffusivity varies as a function of both time and position.